Geochemistry Geophysics Geosystems G3

Article
Volume 13, Number 8
25 August 2012
Q08Z49, doi:10.1029/2012GC004160
ISSN: 1525-2027

Published by AGU and the Geochemical Society

Magnetism of outdoor and indoor settled dust and its utilization as a tool for revealing the effect of elevated particulate air pollution on cardiovascular mortality

Diana Jordanova and Neli Jordanova
Department of Geophysics, National Institute of Geophysics, Geodesy and Geography, Bulgarian Academy of Sciences, Acad. G. Bonchev Str., bl. 3, 1113 Sofia, Bulgaria (vanedi@geophys.bas.bg)

Philippe Lanos
Laboratoire d'Archéomagnétisme, CNRS UMR 5060, CRPAA, Université Bordeaux 3, and UMR 6118, Université de Rennes 1, campus de Beaulieu, FR-35042 Rennes, France (philippe.lanos@univ-rennes1.fr)

Petar Petrov
Department of Geophysics, National Institute of Geophysics, Geodesy and Geography, Bulgarian Academy of Sciences, Acad. G. Bonchev Str., bl. 3, 1113 Sofia, Bulgaria

Tsenka Tsacheva
Institute of Physical Chemistry, Bulgarian Academy of Sciences, Acad. G. Bonchev Str., bl. 11, Sofia 1113, Bulgaria (tsen1956@gmail.com)

[1] Settled indoor and outdoor dusts in urban environment represent an important source of secondary pollution. Magnetic characteristics of the settled dust from six cities in Bulgaria are explored, allowing comparison on a national (country) scale. Monthly variations of the mass-specific magnetic susceptibilities (χ_{indoor}) and ($\chi_{outdoor}$) and calculated dust loading rates for a period of 17 months do not show seasonal variability, probably due to the dominant role of traffic-related emissions and soil-derived particles in the settled dust. The main magnetic mineral is magnetite, present as spherules and irregular particles of pseudo-single-domain grain sizes. Systematically lower remanence coercivities are obtained for outdoor dusts when compared with the corresponding indoor samples, implying that penetration of smaller particles of ambient origin indoors is the main source of the indoor dust. Mean yearly values of the ratio ($\chi_{indoor}/\chi_{outdoor}$) for each city show statistically significant correlation with mortality due to cardiovascular diseases. This ratio reveals the source- and site-specific importance of the anthropogenically derived toxicogenic fraction. Heavy metal content of the settled dust is related to the contribution from several pollution sources (soil-derived, combustion and industrial), discriminated through analysis of principal components. SEM/EDX analyses reveal abundant presence of anthopogenic Fe-containing spherules, irregular particles and diesel exhaust conglomerates. High molecular weight polyaromatic hydrocarbons (PAH) dominate the total PAH content of the outdoor dust samples. The observed linear correlation between total PAH content, coercivity of remanence and the ratio M_{rs}/χ suggest either adsorption of PAHs on iron oxide particles and especially magnetite, or emission related increase in total PAH concentration along with a decrease of effective magnetic grain size of the accompanying magnetic fraction.

Components: 14,100 words, 14 figures, 5 tables.

Keywords: PAH; heavy metals; magnetism; settled dust.

Index Terms: 0345 Atmospheric Composition and Structure: Pollution: urban and regional (0305, 0478, 4251, 4325); 1029 Geochemistry: Composition of aerosols and dust particles; 1512 Geomagnetism and Paleomagnetism: Environmental magnetism.

Received 22 March 2012; **Revised** 6 July 2012; **Accepted** 13 July 2012; **Published** 25 August 2012.

Jordanova, D., N. Jordanova, P. Lanos, P. Petrov, and T. Tsacheva (2012), Magnetism of outdoor and indoor settled dust and its utilization as a tool for revealing the effect of elevated particulate air pollution on cardiovascular mortality, *Geochem. Geophys. Geosyst.*, *13*, Q08Z49, doi:10.1029/2012GC004160.

Theme: Magnetism From Atomic to Planetary Scales: Physical Principles and Interdisciplinary Applications in Geosciences and Planetary Sciences

1. Introduction

[2] Sustainable development and human welfare critically depend on the state of environment. Particular attention is paid on the health effects of atmospheric dust and the role of its elemental composition, grain size and reactivity. The association of PM sizes with health problems represents a scientific and social issue [*Davidson et al.*, 2005; *World Health Organization*, 2006]. A number of epidemiological studies have shown the strong association between PM outdoor concentrations and respiratory symptoms; as well as total, respiratory and cardiovascular mortality [*Pope et al.*, 1995; *Burnett et al.*, 1997; *Pope et al.*, 2002; *Lippmann et al.*, 2003; *Brunekreef and Forsberg*, 2005; *Lippmann*, 2011].

[3] Total amount of settled particulate matter consists of contributions from various sources including soil (crustal material); anthropogenic pollution (motor vehicle emissions, oil and coal combustion, industrial combustion), biomass burning (natural fires) and long-range atmospheric transport. Indoor air quality is also closely related to the outdoor conditions, which makes the estimation of the indoor/outdoor particulate matter (PM) relationships an important parameter for predictions of risk exposure and health effects in urban areas. Conducting long-term monitoring studies on the health effects of particulate matter through direct measurements of PM concentrations is a quite laborious and expensive technique, requiring significant effort and consumables.

[4] One fast and cost effective tool for qualitative estimate of the degree of environmental pollution is magnetometry. Its utilization is based on the presumption that most of the pollutants are accompanied or genetically linked to a fraction of strongly magnetic Fe-containing particulate matter. It is a well established fact, that the waste products and emissions from industrial activities contain among other constituents, a strongly magnetic component [*Gomes et al.*, 1999; *McLennan et al.*, 2000; *Abdul-Razzaq and Gautam*, 2001; *Kukier et al.*, 2003; *Donaldson et al.*, 2005]. Environmentally relevant solid materials such as soils, sediments, dust (atmospheric total suspended particles, particulate matter (PM), road dust), vegetation (leaves, needles, tree rings) serve as carriers of these anthropogenic phases and show enhanced magnetic signal. The use of magnetometry in environmental pollution studies has received increasing attention during the last 15 years. Detailed mineral magnetic characterization of PM10 fraction (particulate matter with aerodynamic diameter less than 10 μm) using filters has been carried out for different locations in Europe and elsewhere [*Muxworthy et al.*, 2001, 2002, 2003; *Spassov et al.*, 2004; *Xia et al.*, 2008; *Sagnotti et al.*, 2006, 2009; *Saragnese et al.*, 2011]. These have shown the importance of anthropogenically produced Fe-oxides in determining the magnetic signature of particulate matter. Vegetation species, growing in a polluted environment are also widely used as a passive biosamplers of atmospheric dust and their magnetic signature reflects the degree of anthropogenic contamination in urban environments [*Matzka and Maher*, 1999; *Hanesch et al.*, 2003; *Jordanova et al.*, 2003; *Lehndorff et al.*, 2006; *Maher et al.*, 2008; *Szönyi et al.*, 2008; *Mitchell and Maher*, 2009]. Road dust has also been a subject of detailed magnetic studies for quantification of the degree of environmental pollution in big cities [*Hoffmann et al.*, 1999; *Goddu et al.*, 2004; *Kim et al.*, 2009;

Figure 1. Schematic map, showing the geographic location of the cities included in the study.

Yang et al., 2010]. Magnetic studies on indoor dust are still rare [*Halsall et al.*, 2008].

[5] The main motivations for undertaking this study are listed below and they aim to resolve several emerging problems in dust magnetism:

[6] a) Most of the studies cited above, report on the magnetic signature of outdoor anthropogenic dust sampled in different ways: (1) active sampling using filters, (2) passive sampling of atmospheric particulates captured on vegetation, and (3) sampling dust settled on roads. Each group of the above mentioned techniques emphasizes on different part of the grain size distribution of the total particulate matter. Dust from filters represents point-specific and usually short-time average of the fine particulate matter (PM10); vegetation surfaces are strongly species-dependent [*Mitchell et al.*, 2010; *Jordanova et al.*, 2010]; and road dust represents mainly traffic-related particulates. Thus, the range of magnetic characteristics, reported in the literature relates to a specific sampling method and deal with outdoor ambient PM.

[7] b) Characterization of indoor dust is needed in order to understand how and to what extent the processes of indoor infiltration and penetration of outdoor particulates influence magnetism – pollution relations. Introducing new proxy magnetic parameters, which may correspond with certain human health indicators would strengthen interdisciplinary epidemiological studies.

[8] c) Naturally deposited on various surfaces above ground, settled dust represents potential source of secondary pollution in the event of re-mobilization of dust particles due to wind storms, artificial ventilation and other ways of mechanical disturbance of deposited dusts. This is the reason for detailed investigation of geochemistry, magnetic signature and health effects of settled dust, both of indoor and outdoor origin.

2. Methods

[9] Settled dust was gathered from indoor and outdoor environments from six big cities in Bulgaria: the capital – city of Sofia, city of Burgas – on the Black sea coast, and other four cities: Russe, Pleven, Stara Zagora and Plovdiv (Figure 1). Information about the localities, their position according to the stationary (point) sources of pollution; surface characteristics and height of the sampling surfaces is given in Table 1. Outdoor localities have been chosen in a way that the surface is sheltered for rain and the corresponding owners (users) of the building do not clean the surfaces and/or disturb dust deposition. The latter requirement is valid for the indoor locations too. The choice of schools as indoor sites was favored by the following conditions: easy access; generally similar building materials and

Table 1. Description of the Sampling Sites

City	Sampling Location	Surface for Dust Loading	Height of the Sampled Surface (cm)	Sampled Area (m^2)	Sample[a]	Distance to the Closest Road (m)	Remarks
Sofia	Supermarket	Window sill	60	2.43	S1o	30	
	Technical university	Window sill	240	3.0	S2o	70	
	101st secondary school "B. Kiro"	top of door keeper cabin	201	2.08	S3i	150	
	Building of telecomun. company	Window sill	200	1.45	S3o	50	Very windy
Burgas	Primary school "E. Pelin"	Glass shelves	200	4.90	B1i 2009	120	300 m between sites 2009–2010
	Secondary school "P. Rosen"	Tops of furniture	210	0.75	B1i 2010	120	
	Post office	Window sill	160	5.1	B1o	120	windy
	Trade Gymnasium	Top of door keeper cabin and café vending machine	200	1.85	B2i	50	
	Casino "King's club"	Window sill	220	2.20	B2o	5	Close to railway station
Russe	Primary school "V. Aprilov"	Top of door keeper cabin	210	1.22	R1i	20	Power plant
	3rd polyclinic	Window sill	160	2.00	R1o	100	Power plant, windy
	Office building	Window sill	160	2.55	R2o	50	
Plovdiv	Seismological station	Window sill	160	0.74	P1i 2009	300	
	Seismological station	Wooden shelf	60	4.0	P1o 2009	300	
	French gymnasium	Tops of furniture	250	2.15	P2i	150	
	Sport hall	Window sill	230	2.30	P2o	20	
	Secondary school "S. Vrachanski"	Café vending machine & shelf	210	1.75	P3i	30	
	Secondary school "7 saints"	Window sills	45	5.1	P3o	30	
	Secondary school "Kl. Ohridski"	Top of door keeper cabin	230	1.98	P4i	100	
	Secondary school "Kl. Ohridski"	Window sills	130	0.77	P4o	100	
Stara Zagora	Mathematics gymnasium "G. Milev"	Entrance shelf	200	3.45	SZ1i	20	
	Mathematics gymnasium "G. Milev"	Window sill	150	1.00	SZ1o	50	
	School of veterinary medicine	Top of door keeper cabin	200	1.37	SZ2i	60	
	School of veterinary medicine	Window sill	150	1.90	SZ2o	60	
Pleven	Primary school "V. Levski"	Top of café making machine	200	0.48	PL1i 2009	250	
	Secondary school "J. Jovkov"	Café vending machine & shelf	200	0.80	PL1i 2010	20	
	Primary school "V. Levski"	Window sill	220	1.30	PL1o	250	
	Secondary school "A. Dimitrova"	Top of door keeper cabin	200	1.50	PL2i	100	Close to railway station
	Secondary school "A. Dimitrova"	Window sill	80	0.60	PL2o	100	Close to railway station
	Office building	Wooden shelf	60	4.0	PL3o	100	Industrial zone

[a]i, indoor; o, outdoor.

construction design of the buildings; available, uncleaned surfaces; absence of significant indoor pollution sources (including smoking); similar temporal changes in pupils' activities (holidays, learning hours, etc.). Having chosen the indoor places in this way, it is considered that indoor pollution is mainly due to the penetration and infiltration of outdoor dust.

2.1. Sampling

[10] Initial planning of the sampling design and distribution of sampling points at each city considered that it would be enough to have two sites per city – one from the central part and another – from clean residential quarter. In the course of monthly sampling, some of the sites, which were initially chosen remained inaccessible many times or become unsuitable due to unforeseen building or renovation works. Therefore, as a final result of the sampling design, 12 pairs of indoor – outdoor sites plus 5 outdoor sites remained available. Pairs of indoor – outdoor places were chosen in a way that their locations are as close as possible. The presence of smooth, possibly non-ferrous surfaces was an important criterion for site selection. Sometimes the lack of under-roof outdoor places at higher elevations caused difficulties. Sampling was carried out monthly during the period May 2009 – November 2010. Three gaps in the time series occur in September 2009, February 2010 and August 2010, when sampling was not performed, but the accumulation continued until the next sampling campaign. Occasionally some data are missing from some locations, where access was not possible (closed buildings due to holidays, etc. on the day of sampling). Dust sampling consisted of brushing carefully an initially cleaned surface of known constant area. Gathered dust material was sealed in plastic bags for laboratory studies.

2.2. Laboratory Measurements and Analyses

[11] Dust samples were air-dried, sieved through 1 mm mesh and weighted using an ABJ 120–4 M Kern analytic balance with precision of 0.1 mg. Magnetic susceptibility of dust material was measured on a MFK-1A Kappabridge (Agico, Brno, Czech Republic) with a precision of 2×10^{-8} SI. When the amount of dust was less than 0.5 g (approx. occupying 1/3 of the volume of a 10 cm^3 cylinder), material was centered in the cylinder in order to avoid incorrect readings. Mass-specific values (χ) were calculated taking into account samples' weight. Magnetic mineralogy was studied by using thermomagnetic analysis of magnetic susceptibility through high-temperature unit of Kappabridge KLY-2 (CS-23 furnace). Changes in magnetic susceptibility at increasing temperatures from 20 up to 700°C was monitored at heating rate of 6.5°C/min (slow heating) in air. Hysteresis loops were measured in applied fields of up to 800 mT for dust samples from June 2009, using a horizontal translation balance at the Palaeomagnetic laboratory (IPGP – Paris, France). Hysteresis parameters: coercive force (B_c), coercivity of remanence (B_{cr}), Saturation magnetization (M_s), Saturation remanence (M_{rs}) and paramagnetic susceptibility (χ_{para}), were calculated. Selected samples have been used for additional magnetic measurements to characterize iron oxides in terms of phase, concentration and grain size. Artificial samples of 0.125 cm^3 were prepared by mixing 0.1 g dust material with gypsum and water in order to fix the grains and impart laboratory magnetic remanences. Stepwise acquisition of Isothermal Remanent Magnetization (IRM) at 30 steps was conducted for identification of magnetic mineralogy using the coercivity spectra. Magnetic remanence measurements were performed with spinner magnetometer JR6A (Agico, Brno) with sensitivity of 2×10^{-6} A/m. Morphology and qualitative elemental composition of single dust particles were examined through SEM – EDX analysis using a JEOL JSM-6390 instrument. Diffraction spectra were analyzed by using INCA program for peak identification (www.x-raymicroanalysis.com). Carbon coating of samples and observations in backscattered electrons mode were used to recognize grains containing high atomic number elements. Analysis of heavy metals content (As, Co, Cr, Cu, Fe, Ni, Pb, Zn) was carried out for fifteen composite samples (mixed dust material from three consecutive months). Elemental analysis was done on dust material dissolved in aqua regia using inductively coupled plasma activation source (Varian Vista-MPX CCD Simultaneous AES ICP). Determination of the concentration of 16 polyaromatic hydrocarbons (PAHs) was carried out for eight samples using gas spectrometer with mass-selective detector GC-MS "Agilent Technologies" – 7890A-GC system, 5975-MSD (USA) equipped with capillary column, and gas spectrometer "Perkin Elmer" model 8310 (USA) equipped with flame ionization detector and capillary column. Weighted dust samples were treated in dichloromethane for 8 h using soxlet extraction apparatus. The samples obtained were filtered and concentrated up to volumes of 0.5–1 cm^3. Aliquots of the filtrates were injected into the spectrometers and quantitative determination of 16 PAHs was obtained.

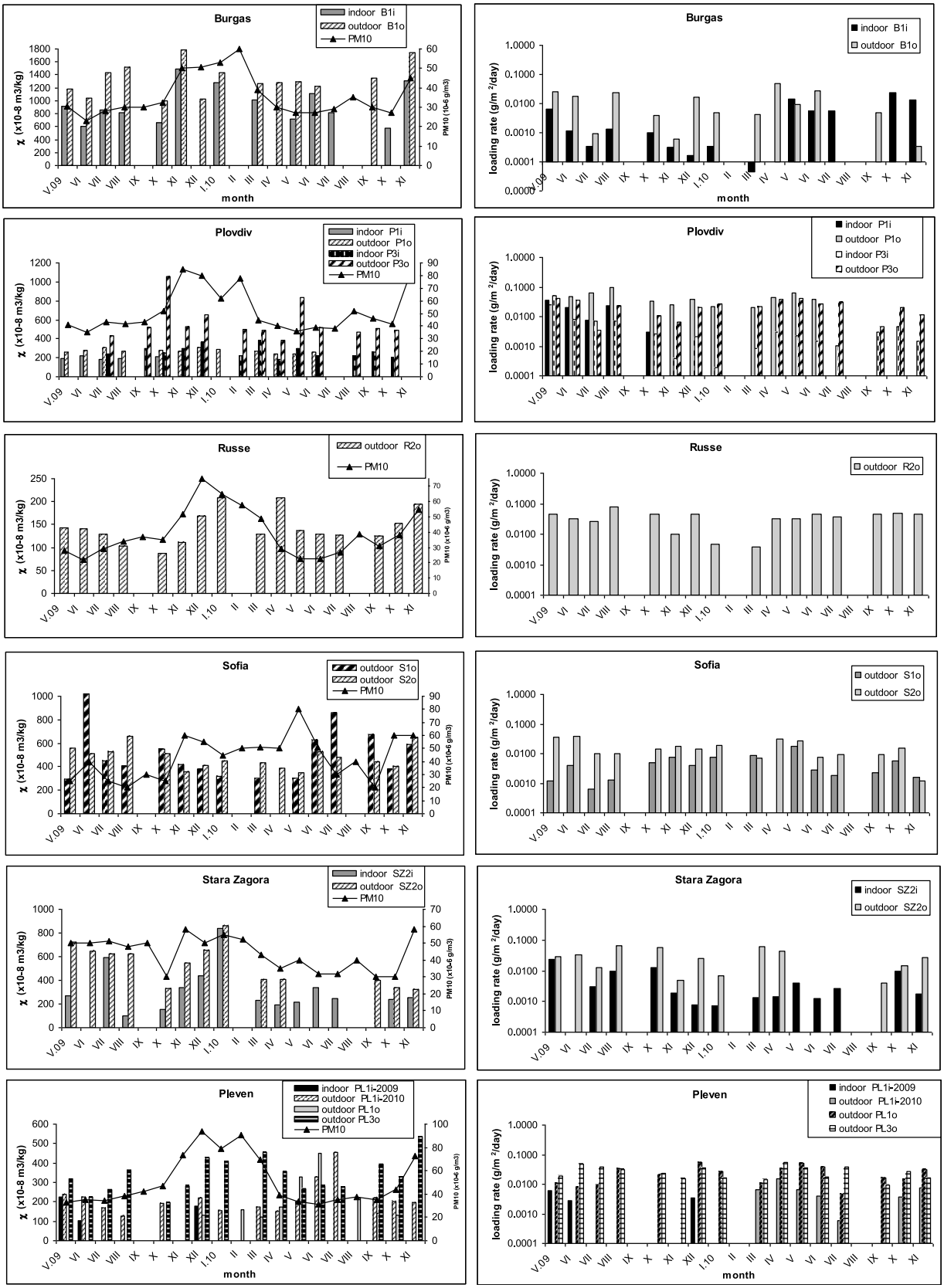

Figure 2. (a) Site-specific variations of magnetic susceptibility (χ) of the outdoor and indoor settled dusts. (b) Monthly variations of dust loading rates for indoor and outdoor sites. Note the logarithmic scale.

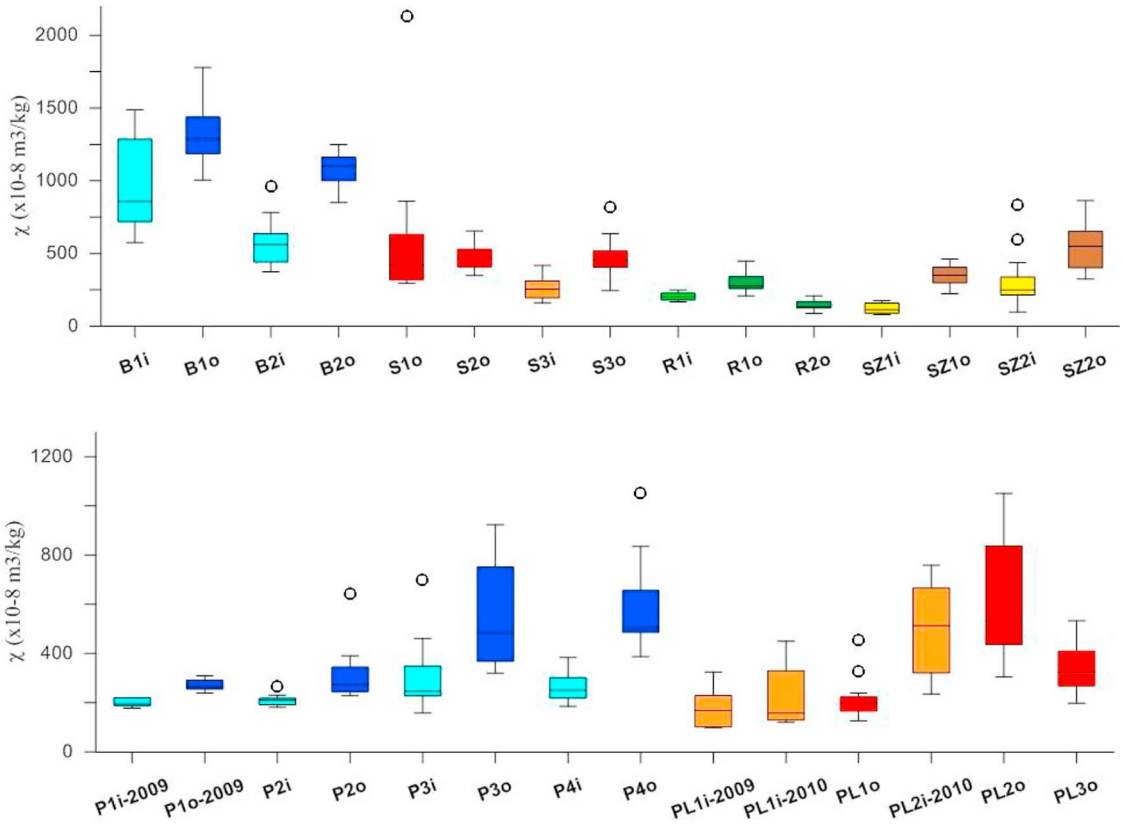

Figure 3. Median values of mass-specific magnetic susceptibility for all sites studied. Outliers are indicated as empty dots. Maximum, minimum, upper and lower quartiles are also shown. Indoor sites are indicated by subscript "i" and given in light color; outdoor sites are indicated by subscript "o" and plotted in dark color.

[12] Microscopic observations on bulk dust material from each month during the period 2009 - spring 2010 were used to estimate the grain size distribution of several indoor and outdoor locations. Number of particles with grain diameters d < 30 μm, 30 μm < d < 50 μm and d > 50 μm was counted. Dynamic Light Scattering (DLS) analysis using 90plus Particle Size Analyzer of Brookhaven Instruments Corp. (USA) with detection range (<1 nm to 6 μm), was carried out on 10 dust samples after ultrasonic dispersion (5 min, 50 W) in distilled water at room temperature.

3. Results

3.1. Magnetic Data

[13] Monthly values of mass-specific magnetic susceptibility (χ) and dust loading rates for the representative pairs of indoor – outdoor locations from the six cities are presented in Figure 2. Records of PM10 concentrations reported for the closest air monitoring station from the national monitoring network in each city are also presented. Systematically higher values of magnetic susceptibility of outdoor samples compared to indoor ones are observed for all pairs. In terms of absolute values, Burgas samples exhibit the highest susceptibilities. Temporal (monthly) variations do not follow seasonality. Weak correlation between monthly magnetic susceptibility values and the amount of PM10 is seen, with better pattern for Stara Zagora and Pleven outdoor sites (samples SZ1o and PL2o). Considering the pattern of dust loading rates in time and space, the situation is more variable. Systematically higher rates of outdoor compared to indoor locations are obtained for the cities of Burgas, Plovdiv, Russe and Pleven. Loading indoor/outdoor rates at Sofia and Stara Zagora vary in time. The highest loading rates are typically observed for Pleven and Burgas sites (notice the logarithmic scale for loading rate in Figure 2). Within-city spatial variations of mean susceptibility values for indoor and outdoor sites studied for the six cities is presented in Figure 3. Using the criteria that the outliers should fall below or above 1.5 times interquartile range plus/minus lower/upper quartile range, several outliers are identified, which are

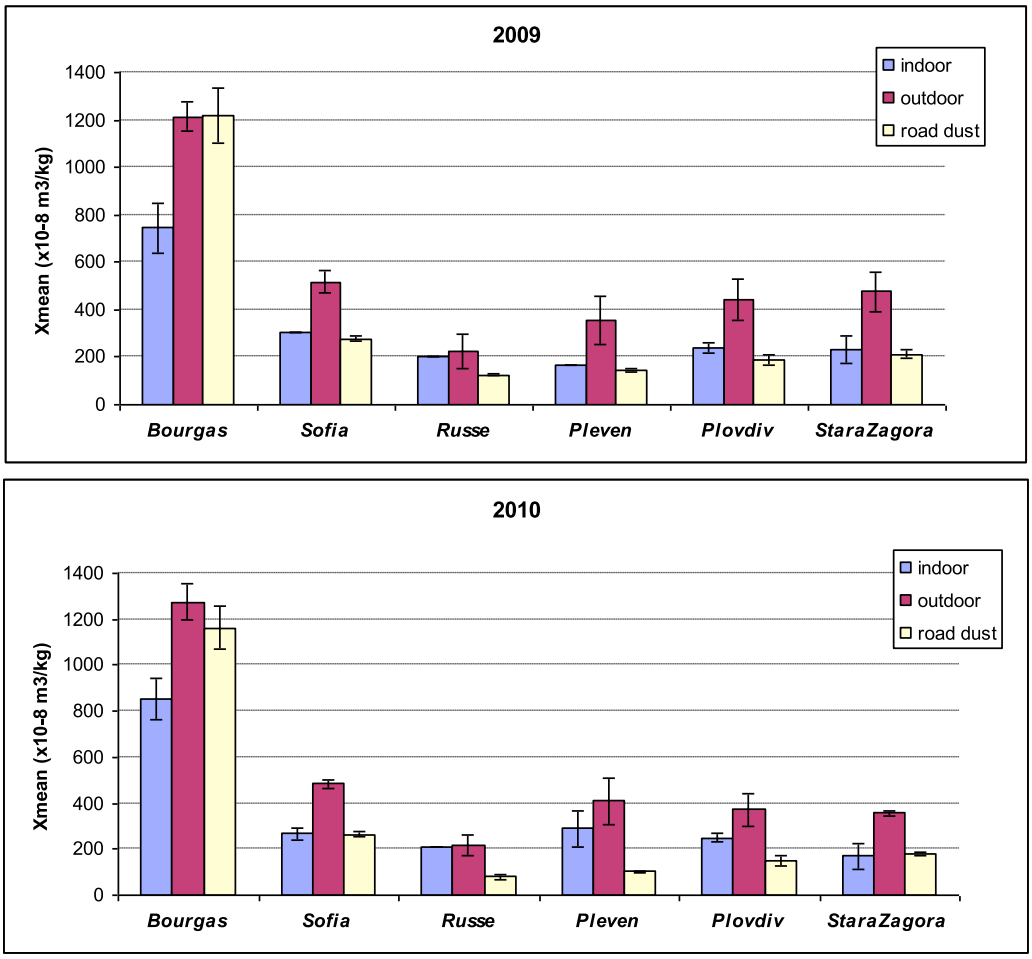

Figure 4. Mean values of indoor, outdoor and road dust per city. Standard deviation of the mean is also plotted.

excluded from calculation of yearly averages based on monthly data sets. Results from Kolmogorov – Smirnov test at 95% significance level suggest that for all samples we have normal distribution of monthly values of magnetic susceptibility (K-S statistics in the range 0.126–0.224 compared to the critical K-S values at $\alpha = 0.05$ of 0.327–0.349). It is observed that the difference between mean indoor – outdoor susceptibilities is the highest for the cities of Burgas and Pleven, which are characterized at the same time with the widest within-sites variations. Mean annual magnetic susceptibilities per city corresponding to the indoor, outdoor and road dusts are presented in Figure 4. Road dust samples are also collected monthly and at the closest roads next to the outdoor sites (detailed results will be published elsewhere). It is obvious from the observed relationships that outdoor dust has as much as twice the susceptibilities of the road dust, except for town of Burgas. Mean indoor susceptibilities are lower than the corresponding outdoor values (Figure 4).

[14] The carriers of magnetic signature in the studied outdoor dust samples are identified through the observed Curie temperatures (T_C) on thermomagnetic χ - T curves (Figure 5). The behavior of the heating curves is quite similar at all locations. Dust samples from Burgas (Figure 5a) show two Curie points – at around 500°C and 600°C. The rest of the samples reveal pronounced Tc at 580°C, with Pleven sample PL2o showing some Tc of 700°C. Cooling curves are always lower than the heating.

[15] In order to check whether high-coercivity magnetic minerals are originally present in our dust samples, stepwise acquisition of IRM is carried out. Representative examples from this experiment are shown in Figure 6. All the samples reveal similar behavior, reaching saturation at relatively low fields of 200–300 mT. Application of strong DC fields higher than 3T does not lead to further increase in the total remanence.

[16] Typical examples of the measured hysteresis loops are presented in Figure 7a. All samples show

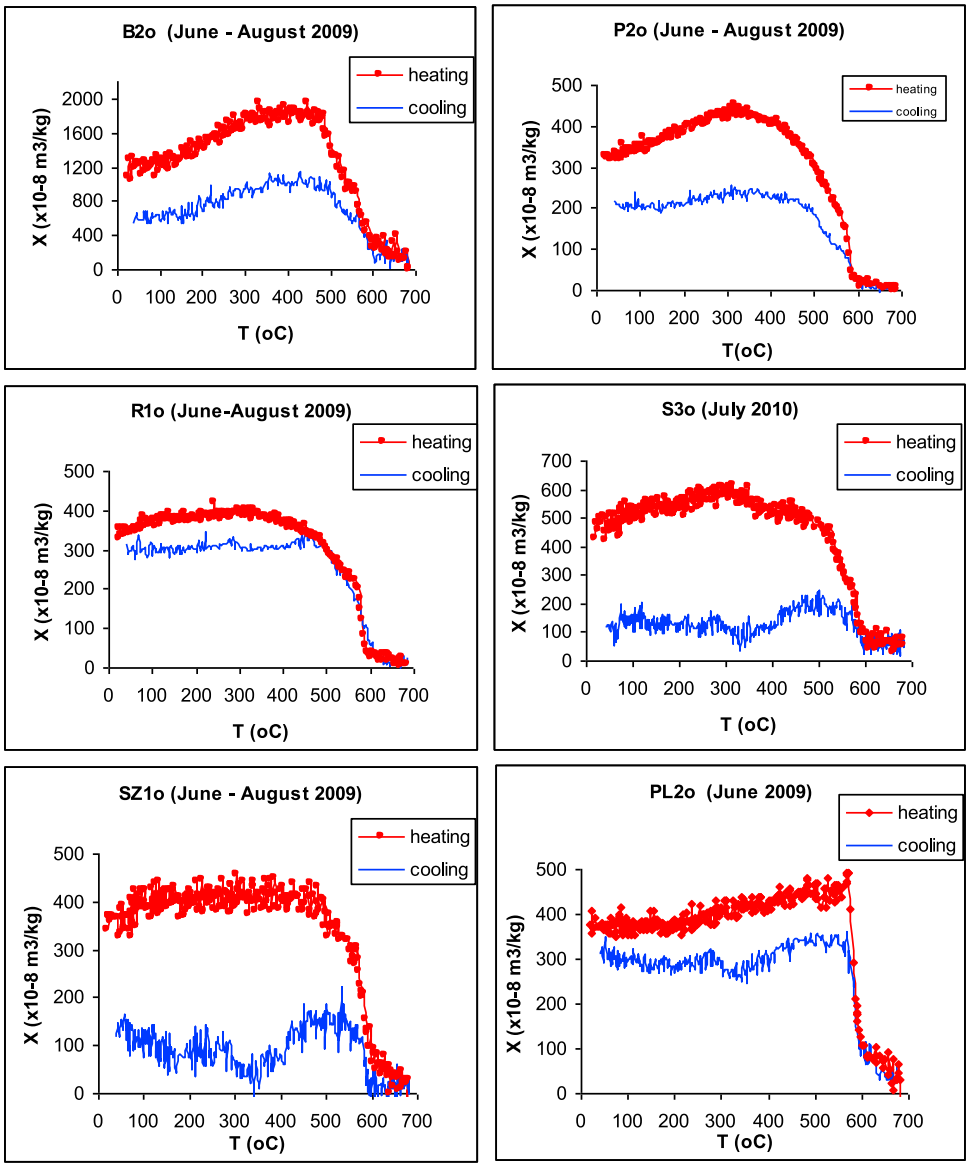

Figure 5. Examples of thermomagnetic analysis of magnetic susceptibility for identification of magnetic mineral phases in the dust samples. Heating is in air using heating rate of 6°C/min.

relatively low coercivities, with loop's closing in fields up to 300 mT. The ratios M_{rs}/M_s and B_{cr}/B_c vary in quite narrow intervals: (0.055–0.1) and (3.08–5.14) respectively. Coercivities (B_c) and coercivity of remanence (B_{cr}) fall in relatively narrow ranges (5.4–10.6 mT and 27.7–38.6 mT). Comparison between sites reveals that indoor dust has higher B_c and B_{cr} than the corresponding outdoor sample. This relationship is opposite for the indoor – outdoor dusts from Stara Zagora and Sofia (samples SZ1i-SZ1o and S3i-S3o in Figure 7b). Calculated from the high-field portion of the loop paramagnetic susceptibility shows systematically higher values for the outdoor sites compared to the corresponding indoor site except that for B1 site (Figure 7c). Effective magnetic grain size as deduced from Day plot [*Day et al.*, 1977] is Pseudo Single Domain (PSD) (Figure 7d).

3.2. Grain Size Analysis of Bulk Indoor and Outdoor Dusts

[17] Relative contribution of the particle number concentrations falling in the three different grain size ranges ($d < 30\ \mu m$, $30\ \mu m < d < 50\ \mu m$ and $d > 50\ \mu m$) is represented on Figure 8. It depicts the predominance of fine grained mode ($d < 30\ \mu m$) in

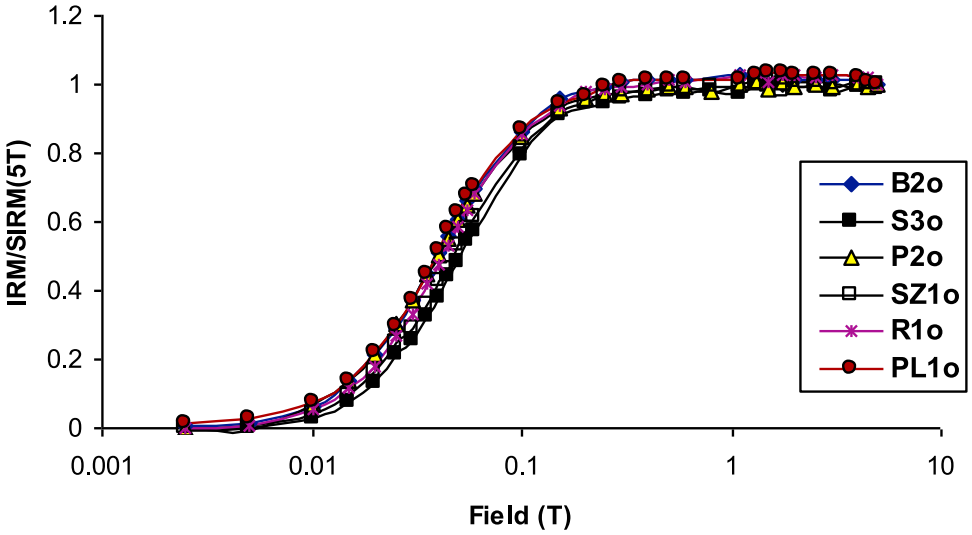

Figure 6. Examples of stepwise acquisition of Isothermal Remanent Magnetization (IRM).

the total grain size distribution. Higher proportion of this fraction in indoor dusts compared to outdoor ones as well as systematically higher percent fines in dusts from 2010 year is observed. As a further constrain within the range (<1–6 μm) the results from DLS analysis indicate the presence of well expressed mode at (1.3–1.8 μm) for both indoor and outdoor samples. In some cases sub-micron fraction with mean hydrodynamic diameter (0.36–0.41) μm is detected (see last column in Table 2).

3.3. SEM Observations and Analysis of Heavy Metal Content

[18] Additional information on the origin of the magnetic signature is obtained from SEM observations on single grains and EDX-spectra. Microphotographs of typical particulate matter from outdoor dust are shown in Figure 9. A panoramic view of the dust from sample SZ1o gathered in May 2009 (Figure 9a) reveals the presence of both soil-derived irregular particles as well as anthropogenic ones. Closer views of such anthropogenic spherules from combustion processes are shown in Figures 9b and 9d. In samples from spring and summer months a wealth of pollen grains with adhered dust particles on their surfaces are observed. One example of pollen grain from Sofia (locality S3o) is given in Figure 9c.

[19] Results from the analysis of elemental heavy metal (HM) content in composite dusts from three summer months (June–August 2009) are given in Table 2. The highest concentrations of all studied elements are obtained for the outdoor dust from the city of Burgas (B2o and B1o). Especially remarkable are the contents of As, Cu and Pb. Tomlinson Pollution Load Index PLI [*Angulo*, 1996] has been calculated, taking the outdoor site R2o from Russe as a site representative of an urban background, since it shows the lowest concentrations of heavy metals. PLI index, using concentrations of the heavy metals given in Table 2 except Fe, is calculated as:

$$PLI = \sqrt[n]{CF1xCF2x.....CFn}, \text{ where } CF_{metal} = \frac{Cmetal}{Cbackground}.$$

[20] Iron is excluded from the calculation in order to avoid dependency between magnetic and non-magnetic parameters, used for further comparisons. Statistical analysis of heavy metal data and magnetic susceptibility was carried out using STATISTICA 8 software. Cluster analysis identified the presence of two clusters with members of the first cluster – samples from Burgas, and the second cluster (cluster 2) contained all the other samples. Cluster means for different variables are well separated (Figure 10a), which lead us to consider further correlations among heavy metals and magnetic susceptibility within samples classified in each cluster separately. Source identification of heavy metals in the dust samples from cluster 2 was attempted using principal component analysis of standardized (Varimax normalized) variables. Results indicate that three factors with eigenvalues higher than 1, account for 75.4% of the overall variance (Table 3). Factor 1 has high loadings for Fe, Mn and χ, explaining 40.6% of the variance; Factor 2 – Pb, As and PLI accounting for 21.3% of the total variance; and Factor 3 contains

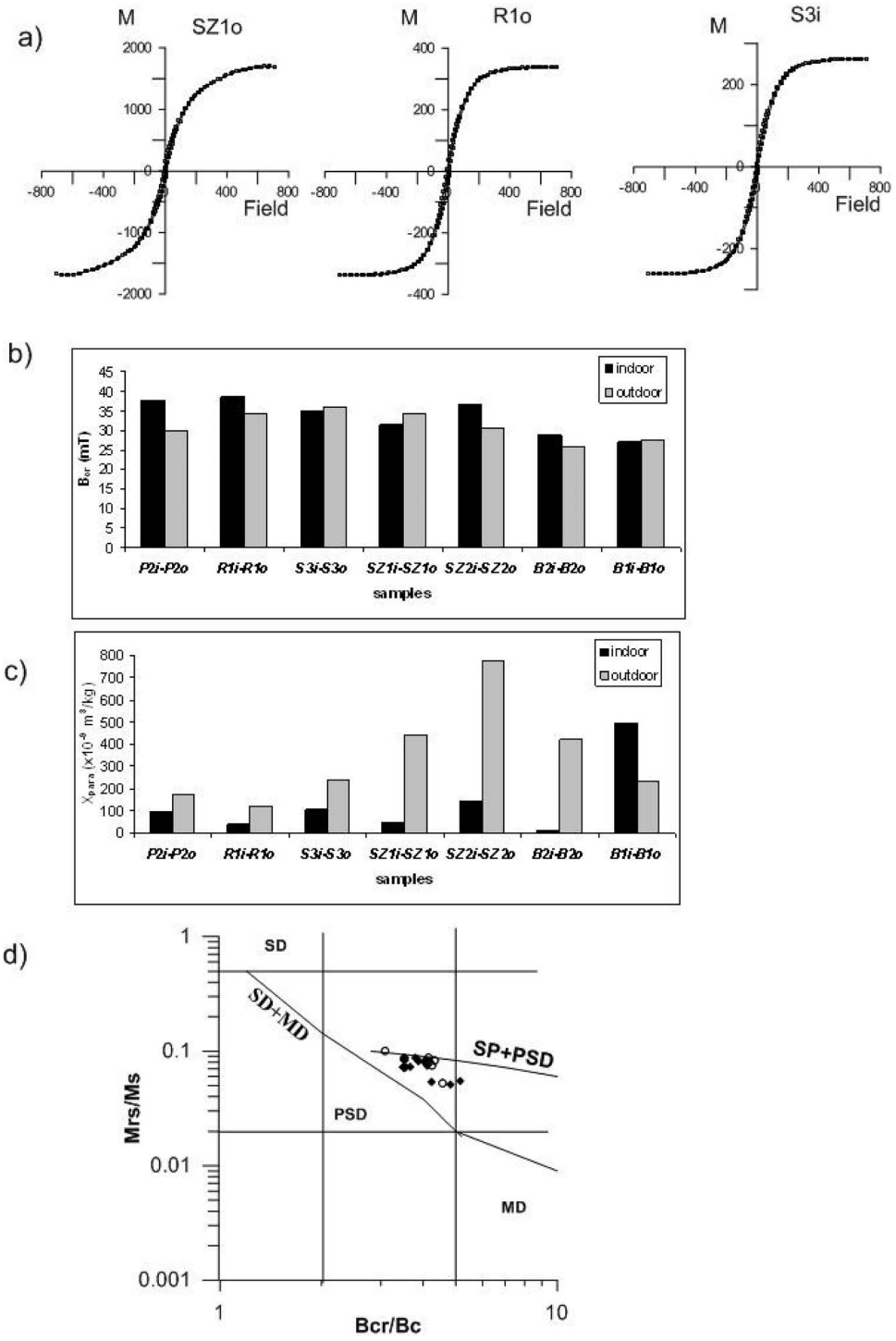

Figure 7. (a) Examples of typical hysteresis loops, obtained after subtraction of the paramagnetic component. Maximum field: 800 mT. Magnetization in 10^{-6} Am^2/kg. (b) Comparison between the coercivity of remanence (B_{cr}) for the pairs of indoor – outdoor dusts. (c) paramagnetic susceptibility (χ_{para}) for the pairs of indoor – outdoor dusts. (d) Day plot [*Day et al.*, 1977] for identification of the effective magnetic grain sizes. Mixing curves from *Dunlop* [2002] for SD + MD and PSD + SP particles are also shown.

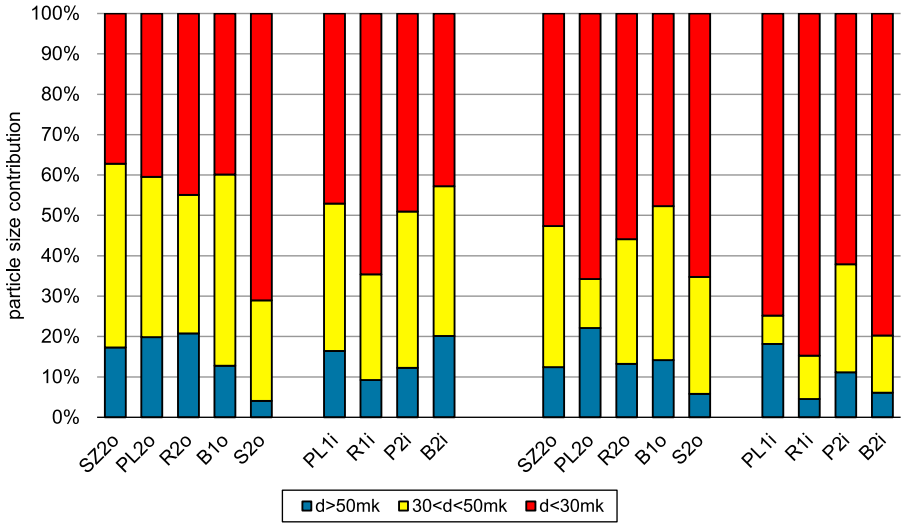

Figure 8. Relative number of mineral particles in three grain-size ranges: d > 50 μm; 30 μm < d < 50 μm and d < 30 μm.

Co and Cr with 13.6% explained. Table 4 shows the correlation coefficients among variables.

3.4. PAH Data

[21] Analysis of PAHs in eight samples from outdoor locations (Table 5) gives information about dust contamination with toxic organic compounds. Among the 16 measured PAHs (U.S. EPA's priority compounds), no extreme concentrations are identified. The highest total PAH content is obtained for the outdoor dust from the towns of Russe (R1o) and Stara Zagora (SZ1o). Considering the relative abundance of different species, high molecular weight 5-ring PAHs give the highest contribution to the total content – benzo(b, k)fluoranthene (BbF, BkF) and dibenz(a)anthracene (DaA). Anthracene (3-ring PAH) has systematically higher contribution in most of the samples. Exploring the relationships between total PAH content and magnetic parameters measured within this study, we found the existence of linear correlations between total PAH content on one side, and M_{rs}/χ and B_{cr}, on the other (Figure 11).

Table 2. Results From the Heavy Metal Analyses (in mg/kg)[a]

Sample	As	Co	Cr	Cu	Fe	Mn	Ni	Pb	Zn	PLI	0–5 mk GSD Peaks	
B2o	591.2	13.5	71.2	5447.7	27994	542.5	38.1	1665.2	2079	11.28	0.36	1.68
B1o	25.7	16.1	64.6	753.6	28373	695	33.7	138.7	578.2	3.81		
S2o	9.2	9.8	66.9	200.8	17140	629.3	31.7	162.5	598.4	2.69		
S3o	13.3	6.7	48.6	190.8	21106	565.6	31	94.3	916.9	2.49		1.43
PL1o	10.7	5.2	39.2	153.4	12182	309.8	25.4	122.7	725	2.02		
PL2o	8.95	5.95	50.35	111.05	16575	328.95	31.8	104.2	1114.85	2.13		1.43
R2o	3	5	32.4	77.5	10472	238.5	22.5	22	206.2	1.01		
R1o	7.3	7.1	42.5	117.2	13859	266.7	26.3	139	4522.4	2.46		1.27
P2i	13.7	6.2	57.8	185.3	12496	363.2	40.3	187.7	985	2.71		1.97
P2o	10.9	7.3	49.6	152.5	14770	291.3	35	409.85	12890.5	3.75	0.41	
P3o	18.8	6.7	47.9	180.5	16083	334.7	29.5	677.6	1464.5	3.25		
P4o	15.3	5.2	37.1	112.7	12976	411.5	33.8	304.3	3425.3	2.95		
SZ1i	10	7.4	81	84.3	10493	292	20.8	231.1	1971.7	2.52		1.83
SZ1o	12.8	7.1	37.1	124.1	16161	402	27.6	139.5	674.6	2.18		1.60
SZ2o	11.1	7.6	46.1	141.8	20186	454.3	25.3	101.6	829	2.24		

[a]Site R2o is a background site at the city of Russe, which shows minimum concentration of the measured heavy metals and is used for the calculation of PLI index. The last two columns show peaks in grain size distribution (GSD) of mineral particles in the range 0–5 μm, observed by Dynamic Light Scattering. Samples represent composite material from the months June-July-August 2009.

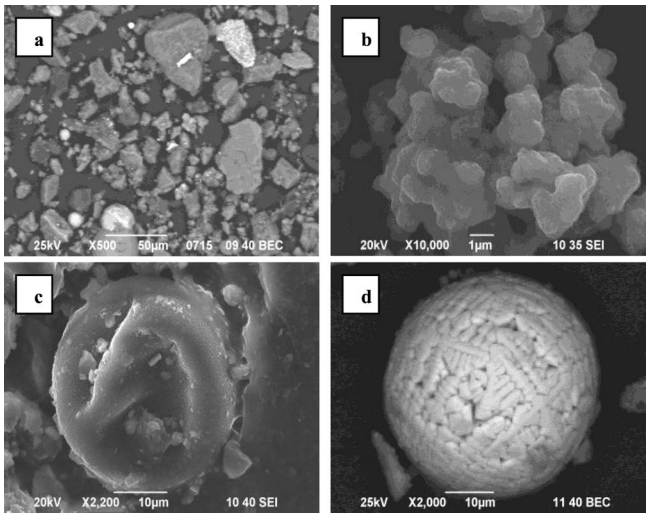

Figure 9. Scanning electron microscopy photographs, showing typical morphology of the anthropogenic magnetic fraction in the dust samples. (a) Panoramic view of the magnetic extract of dust material from site SZ1o (May 2010). (b) cluster of Fe-containing spherical particles, probably from diesel exhaust emissions. (c) pollen grain from site S2o (Sofia, May 2009). (d) Fe-containing anthropogenic spherule from site SZ1o (May 2010).

3.5. Magnetic Susceptibility, the Ratio $\chi_{indoor}/\chi_{outdoor}$ of the Settled Dust and Health Indicators

[22] Current state of research in environmental pollution studies favors utilization of easily measurable magnetic parameters such as magnetic susceptibility (χ) and Isothermal remanence (M_{rs}) as good proxies for the degree of heavy metal pollution and PM load [*Hoffmann et al.*, 1999; *Muxworthy et al.*, 2001; *Kim et al.*, 2007; *Maher et al.*, 2008; *Mitchell and Maher*, 2009; *Yang et al.*, 2010]. Most of the studies report data concerning one city (e.g., single location), where various relative contribution from different pollution sources determine heavy metal – magnetism relationship. However, on a large spatial scale, where we have different lithogenic background and various long distance pollution transport (transboundary pollution), one could not expect a single relationship. This requires introduction of a ratio or other parameter, which effectively can account for the above mentioned factors and reveals a common pollution – magnetism link. In general, we can consider urban dust as a mixture of: lithogenic (soil)

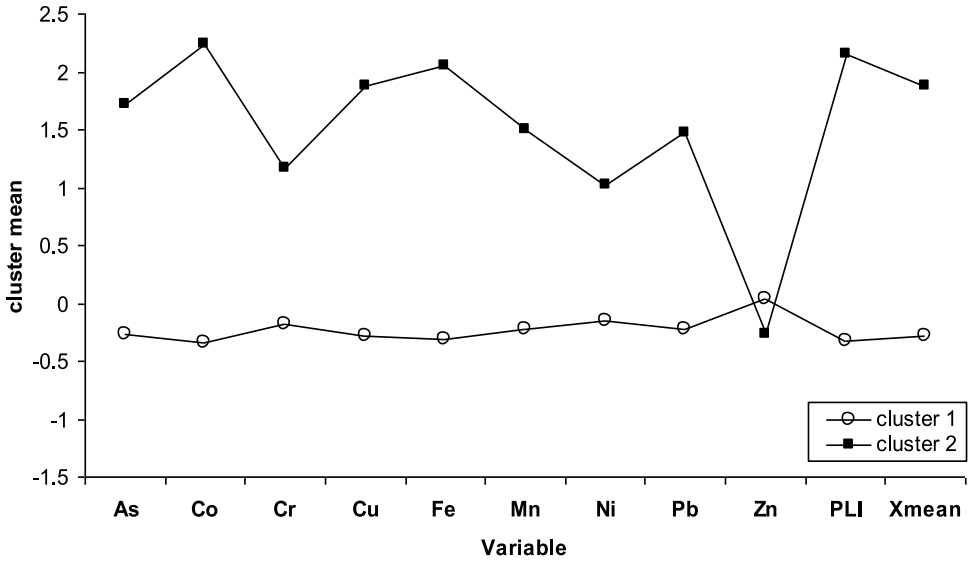

Figure 10. Cluster means for all variables.

Table 3. Calculated Factor Loadings, Eigenvalues and Explained Variance for Dust Samples From the Second Cluster (All Data Excluding Burgas Sites)

Factor	Eigenvalue	% of the Total Variance	Cumulative %	Factor Loadings (Varimax Normalized)
1	4.461	40.56	40.56	Fe – 0.922 Mn – 0.797 χ – 0.81
2	2.342	21.29	61.85	As – 0.845 Pb – 0.927 PLI – 0.647
3	1.493	13.57	75.42	Co – 0.717 Cr – 0.968
4	0.99	8.99	84.42	Ni – 0.92 Cu – 0.607
5	0.919	8.36	92.78	Zn – 0.967

component; anthropogenic (combustion) component; re-suspended road dust component; and long-distance pollution component. Each of these components has different grain size distribution with the finest one connected to combustion, and coarsest one to soil derived and re-suspended particles [*Morawska and Salthammer*, 2003]. Recent studies further clarify experimental grain size distribution data of soil derived mineral dust [*Zhang et al.*, 1998; *Goossens and Buck*, 2011]. The main grain size mode of local sources is represented by the silt fraction 5–60 μm with maximum depending on the grain size of the eroding substrate but usually having clearly expressed peak at 15 μm for sand units and 50–70 μm for silty and clayey units [*Goossens and Buck*, 2011]. Critical role is played by the organic content, which leads to formation of soil aggregates and diminishes the net erosivity of the soils [*Aimar et al.*, 2012]. Anthropogenic emissions of primary importance in urban environment are coming from traffic-related sources: combustion-derived and non-exhaust [*Morawska et al.*, 2008; *Thorpe and Harrison*, 2008]. Their particle size distribution is often bi-modal, comprising ultrafine fraction (PM < 1 μm) and coarse fraction (PM2.5–10 μm). Larger particles are emitted also from industrial combustion processes, but they are heavier and deposit fast close to the source. Theories and modeling of dry deposition of mineral dust aerosol [*Marticorena and Bergametti*, 1995; *Foret et al.*, 2006] show that coarse particles with aerodynamic diameter more than 20 μm are only limited to the so-called "saltation layer" with maximum vertical extends of the particle trajectories of about 1 m. Thus, dust sampling surfaces at higher heights in our study (see Table 1) would preferentially catch smaller particles of anthropogenic origin. Strongly magnetic particles in the total dust obey the same laws but have smaller physical sizes due to the effect of higher density of magnetite as compared to the usual "nominal" density of 2.56 g/m^3 considered in model calculations.

[23] Establishment of a "background" value characterizing magnetic susceptibility of non-polluted urban environment requires high-density spatial sampling for each city. We applied another approach, assuming that the indoor dust represents fine-grained fraction of the outdoor dust, which is able to penetrate inside buildings forced by natural air exchange, human activities and infiltration through buildings' openings and cracks [*Chen and Zhao*, 2011]. This supposition is valid only if the indoor space is free of dust sources, which could be postulated for the entrances of the schools. Thus, we calculate the ratio of indoor to outdoor susceptibilities ($\chi_{indoor}/\chi_{outdoor}$) as an estimate for the importance of traffic-related and industrial pollution to the indoor air quality. Official statistical information, which is provided on the Web site of the Bulgarian National Statistical Institute (www.nsi.bg), is used as a source data for

Table 4. Correlation Coefficients Among Variables for Cluster 2 Data Set[a]

	N = 13 (Casewise Deletion of Missing Data)										
Variable	As	Co	Cr	Cu	Fe	Mn	Ni	Pb	Zn	PLI	Xmean
As	1.00	0.01	0.06	0.53	0.31	0.29	0.46	**0.70**	0.01	**0.66**	**0.57**
Co	0.01	1.00	**0.60**	0.43	0.45	**0.58**	0.03	0.09	0.11	0.37	0.51
Cr	0.06	**0.60**	1.00	0.18	−0.05	0.23	0.03	0.13	0.00	0.33	−0.01
Cu	0.53	0.43	0.18	1.00	0.55	**0.65**	**0.59**	0.29	−0.02	0.49	**0.59**
Fe	0.31	0.45	−0.05	0.55	1.00	**0.71**	0.20	−0.03	−0.09	0.20	**0.71**
Mn	0.29	**0.58**	0.23	**0.65**	**0.71**	1.00	0.29	−0.14	−0.30	0.17	**0.59**
Ni	0.46	0.03	0.03	**0.59**	0.20	0.29	1.00	0.27	0.30	**0.58**	0.20
Pb	**0.70**	0.09	0.13	0.29	−0.03	−0.14	0.27	1.00	0.41	**0.77**	0.52
Zn	0.01	0.11	0.00	−0.02	−0.09	−0.30	0.30	0.41	1.00	**0.66**	0.03
PLI	**0.66**	0.37	0.33	0.49	0.20	0.17	**0.58**	**0.77**	**0.66**	1.00	0.50
Xmean	**0.57**	0.51	−0.01	**0.59**	**0.71**	**0.59**	0.20	0.52	0.03	0.50	1.00

[a]Significant at p > 0.05 correlations are highlighted in bold.

Table 5. Concentration of the Measured 16 PAHs (mg/kg) for the Outdoor Dusts and Isomer Ratios for Source Identification [*Yunker et al.*, 2002][a]

			Russe				Stara Zagora		
Compound	Acronym	Burgas: B2o	R1o	R2o	Plovdiv: P2o	Pleven: PL2o	SZ1o	S2o	Sofia: S3o
Naphtalene	NP	0.040	0.568	0.013	0.113	0.180	0.191	0.109	0.131
Acenaphtene	ACE	0.030	0.058	0.346	0.052	0.112	0.009	0.016	0.044
Acenaphtilene	ACY	0.085	0.187	0.020	0.039	0.071	0.036	0.055	0.038
Fluorene	FL	0.013	0.284	0.010	0.010	0.113	0.007	0.088	0.030
Phenantrene	PHE	0.042	0.377	0.061	0.029	0.148	0.067	0.084	0.122
Anthracene	ANT	0.148	0.507	0.372	0.064	0.351	0.610	0.117	0.889
Fluoranthene	FLA	0.002	0.250	0.163	0.025	0.077	0.044	0.043	0.011
Pyrene	PYR	0.002	0.260	0.029	0.001	0.090	0.062	0.005	0.026
Benzo(a)anthracene	BaA	0.003	0.014	0.037	0.003	0.124	0.051	0.053	0.258
Chrizene	CHR	0.003	0.013	0.004	0.025	0.069	0.119	0.052	0.059
Benzo(b)fluoranthene	BbF	0.007	5.000	0.007	0.005	1.004	0.062	0.006	0.180
Benzo(k)fluoranthene	BkF	0.008	0.028	0.128	0.085	0.009	0.388	0.015	1.080
Benzo(a)pyrene	BaP	0.165	0.041	0.177	0.040	0.231	0.082	0.078	0.140
Indenopyrene	IP	0.008	0.024	0.325	0.136	0.012	0.187	0.007	0.222
Dibenz(a,h)anthracene	DahA	0.013	0.064	2.652	0.297	0.473	4.782	0.174	2.482
Benzo(g,h,i)perylene	BghiP	0.006	0.632	0.009	0.006	0.028	0.013	0.387	0.010
SUM PAH	PAHtotal	0.575	8.306	3.629	0.930	3.092	6.135	1.341	5.046
ANT/(ANT + PHE)	R178	0.763	0.570	0.857	0.738	0.566	0.902	0.489	0.800
FLA/(FLA + PYR)	R202	0.989	0.670	0.696	0.722	0.819	0.933	0.730	0.987
BaA/(BaA + CHR)	R228	0.403	0.951	0.440	0.326	0.420	0.545	0.086	0.093

[a]Samples represent composite material from the months June-July-August 2009.

mortality indices. Mean annual values of $\chi_{indoor}/\chi_{outdoor}$ ratio have been calculated for each sampling pair and each city with the corresponding standard deviations. The same procedure was utilized for obtaining mean annual susceptibility values. These mean data are compared with the official statistical data for mortality cases resulting from respiratory diseases (including pneumonia, chronic pulmonary diseases, asthma and influenza) as well as cardiovascular diseases. Figure 12 shows the relationship between indoor and outdoor mean susceptibilities with the two mortality indices. For both medical indices and both indoor and outdoor susceptibilities, there is no statistically significant correlation even though one does not consider data points for Burgas (site with the highest susceptibilities). On the other hand, Figure 13 depicts the relationship between the ratio $\chi_{indoor}/\chi_{outdoor}$ and mortality caused by the two factors. No significant correlation is revealed between $\chi_{indoor}/\chi_{outdoor}$ and mortality caused by respiratory diseases (Figure 13a). The observed relationship between $\chi_{indoor}/\chi_{outdoor}$ and mortality due to cardiovascular diseases in Figure 13b is fitted by linear regression. Standard method for calculating regression equation without considering the error bars was applied, resulting in R^2 of 0.82 at $p < 0.001$

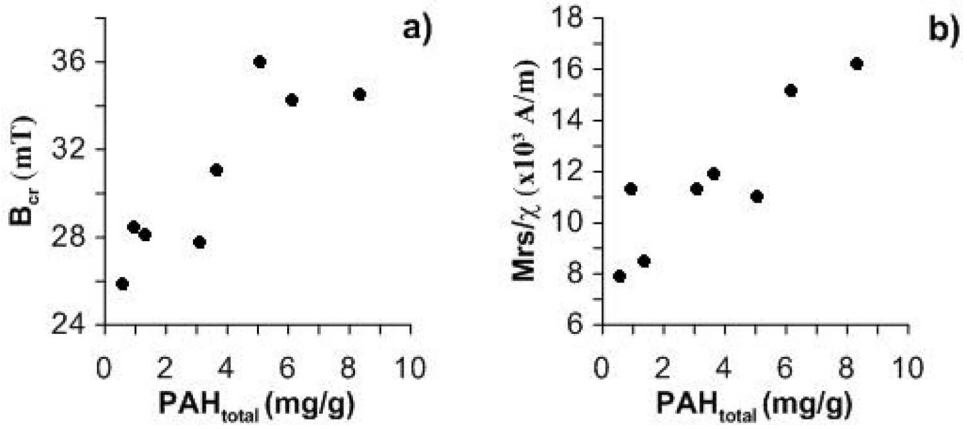

Figure 11. Relationship between total PAH content and (a) coercivity of remanence B_{cr} and (b) ratio M_{rs}/χ.

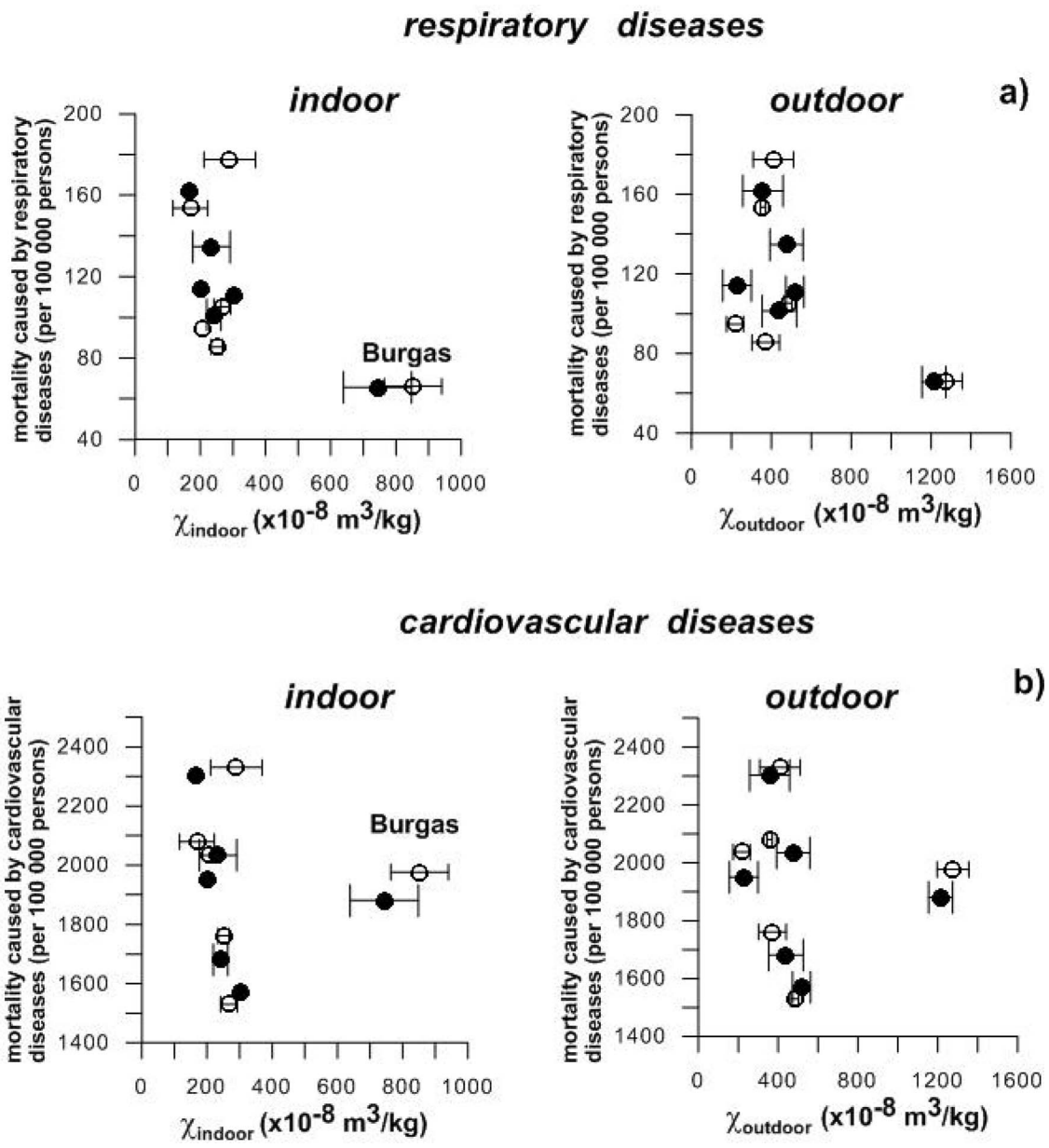

Figure 12. Relationship between the mean annual values of outdoor and indoor magnetic susceptibilities for 2009 and 2010 and mortality due to (a) respiratory diseases (per 100 000 persons) and (b) cardiovascular diseases (per 100 000 persons). Error bars represent the estimated standard deviations for the corresponding mean values.

significance level. Confidence intervals for the two parameters of the regression equation (slope and intercept) were calculated (Figure 14a). Experimental errors in determination of the ratio $\chi_{indoor}/\chi_{outdoor}$ have been taken into account by using RenCurve software, originally developed for the purposes of archaeomagnetic dating [*Lanos*, 2004]. Here, the age is replaced by $\chi_{indoor}/\chi_{outdoor}$ and field element (D, I or Jn) – by the mortality index with certain scaling in order to get similar range of values. Application of the Bayesian statistic on the data results in calculation of the Highest Posterior Density (HDP) envelope at 95% level. Density distribution within the envelope is represented on Figure 14b.

4. Discussion

[24] The subsequent discussion is structured so as to provide insights on: 1) how and why the amount of dust and its magnetic signal reflects temporal and lateral changes in environmental conditions; ii) which magnetic minerals are responsible for the magnetic signature and what are their grain sizes;

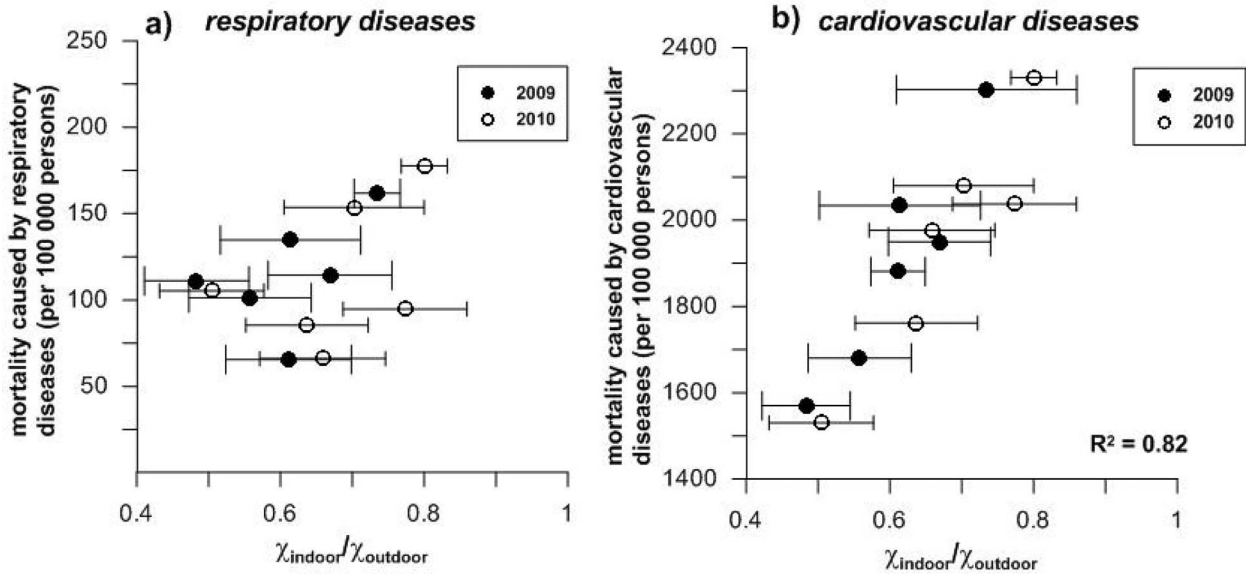

Figure 13. (a) Relationship between the mean annual values for 2009 and 2010 of the ratio $\chi_{indoor}/\chi_{outdoor}$ and mortality (per 100 000 persons) caused by respiratory diseases for the six cities. (b) Relationship between $\chi_{indoor}/\chi_{outdoor}$ and mortality (per 100 000 persons) caused by cardiovascular diseases. Error bars represent the estimated standard deviations for the corresponding mean values.

iii) what is the relationship between dust magnetism and the content of major heavy metals and PAHs which would justify the utilization of magnetic parameters in health studies; iv) review of physical background, epidemiological and toxicological studies on the role of mineral dust and especially iron oxides for human health; and v) testing the validity and reliability of the magnetic ratio $\chi_{indoor}/\chi_{outdoor}$ as a tool for estimation of cardiovascular diseases caused by urban pollution.

4.1. Site-Specific and Temporal Variations of Mass-Specific Magnetic Susceptibility and Dust Loading Rates

[25] Mass-specific magnetic susceptibility (χ) as one basic magnetic characteristic of the solid

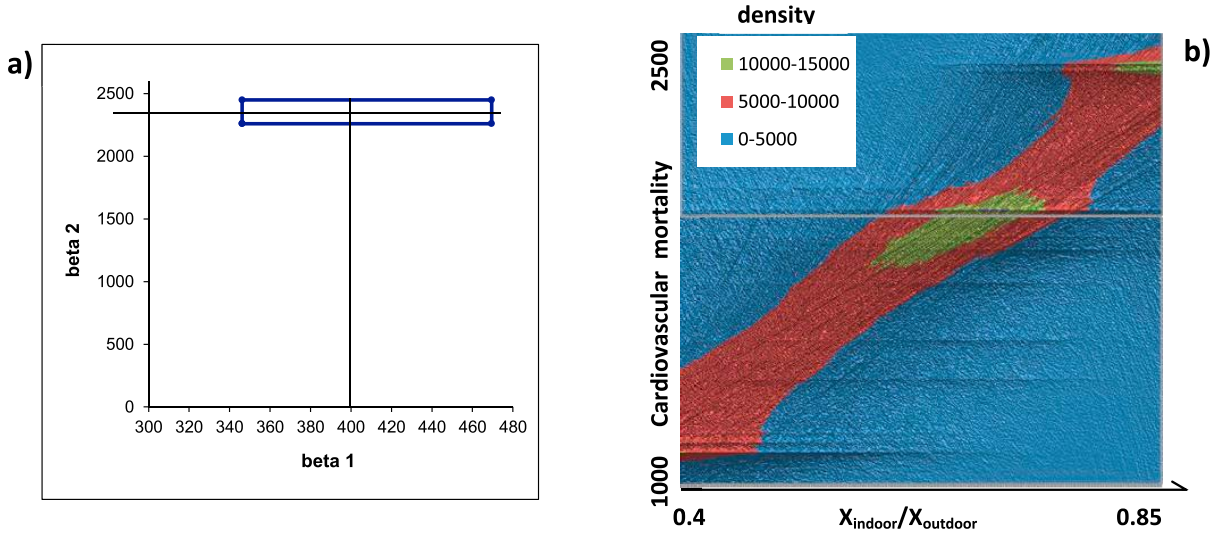

Figure 14. Area defined by the estimated confidence intervals for the intercept (beta 1) and slope (beta 2) of the regression equation, representing linear regression of the ratio $\chi_{indoor}/\chi_{outdoor}$ and cardiovascular mortality.

matter, depends generally on the mineralogy, concentration and grain size of strongly magnetic Fe-oxides in the material [*Dunlop and Ozdemir*, 1997]. In this context, settled dust in urban areas has a magnetic signature, which is determined by the cumulative effect of the magnetic fractions, inherent to its various components. Temporal and lateral changes of the magnetic susceptibility at a given location thus, are indicative about any changes in the relative proportion of the different fractions, or changes in the dust sources. Magnetic measurements are capable of identifying even subtle changes in the content of strongly magnetic Fe-oxides down to 50 ppm (titano)magnetite [*Dearing*, 1999]. Thus, monthly variations of χ shown in Figure 2 represent a sensitive record of changing mineral content in the outdoor and indoor settled dusts. Systematically lower indoor values suggest decreases in the relative proportion of strongly magnetic iron oxides in the total mineral dust. Gravitational settling is the major process of coarse dust dynamics, forcing sedimentation of coarser and heavier particles close to the origin [*Fisher and Macqueen*, 1981]. The amount of outdoor Fe-oxide particles, which belong to the heavy mineral fraction, will depend on their size distribution. The observed systematically lower indoor susceptibilities as compared to their outdoor counterparts in Figure 2, suggests that the major source of indoor dust is the penetration of outdoor dust inside by means of diffusion, turbulent flows through open windows (doors) and mechanically introduced dust by people's activities. The absence of correlation between monthly mass-specific susceptibility and PM10 concentrations for most of the sites implies that the main contribution to the magnetic signature of the settled dust is coming from traffic and re-suspended road dust, as far as seasonality in PM10 is generally explained by higher emissions from combustion related to heat production (domestic burning, power plants, etc.). There are different cases, reported in the literature, some of them showing clear seasonal trends in PM and its magnetic susceptibility [*Muxworthy et al.*, 2003; *Kim et al.*, 2007], and others do not show this. For example, no seasonal changes in the coarse PM10 contents are observed by *Liu and Harrison* [2011] in a study of dust from UK, which is explained by the predominantly traffic-related sources. Temporal changes of dust loading rate (Figure 2b) indicate higher sedimentation outdoors than indoors, thus proving our concept that indoor dust sources can be neglected. A particular case is Sofia site S1o and partly SZ1o, which are characterized by lower outdoor dust loading rates as compared to indoor ones. This can be explained by the permanently windy microclimate conditions at these sites, mentioned in Table 1. The range of variation in dust loading rate is well within typical loading rates reported for settled dust [*Maertens et al.*, 2004]. Taking the monthly average loading rates, mean dust load per year is calculated. We obtained values between 6 and 15 g/m^2/yr. The highest dust load is calculated for Stara Zagora and especially high value of 71 g/m^2/yr for the outdoor site in the city of Pleven - PL2o. As far as we have chosen the entrances of public buildings (mainly schools) for indoor places (Table 1), there should be little or no effects of indoor PM sources on the amount and characteristics of the total settled dust.

[26] The relative importance of temporal susceptibility changes for each sampled site is represented by the median, lower and upper quartile ranges of χ in Figure 3. The largest variability is observed for the indoor and outdoor dusts from Burgas, and outdoor settled dusts from Pleven and Plovdiv. Using t-test statistics, significant difference at $\alpha = 0.05$ level between mean χ values of indoor and outdoor sites per each city, is proved. An impression on the absolute differences in magnetic susceptibility of settled dusts from the six cities provides Figure 5. Direct comparison among signals from indoor, outdoor and road dusts implies that except for Burgas, outdoor dust is far much enriched with magnetic fraction as compared to the other two dusts. This finding indicates that fine grained magnetic fraction from anthropogenic activities is settled at higher elevations than the road level but is not fine enough to penetrate (infiltrate) effectively indoors. The exact indoor – outdoor (I/O) ratio would then depend on the particular grain-size distribution of the ambient dust and its aerodynamic behavior. The almost equal values obtained for mass specific magnetic susceptibility of road dust and outdoor dusts from Burgas suggest that in this case coarse-grained soil-derived magnetic particles dominate the total settled dust material.

4.2. Magnetic Mineralogy and Grain Size of the Settled Dust

[27] Further implications of magnetic signature to environmental pollution need to take into account the type and grain size of the main magnetic minerals contributing to the signal. A suitable tool for this purpose is thermomagnetic analysis of susceptibility (Figure 4). Similar shapes of the heating curves except B2o site imply that the collections of settled dust are characterized by uniform

magnetic mineralogy, originating from both local soil dust component and magnetic fraction of the anthropogenic emissions. All curves show the most pronounced decrease of the signal at about 580°C, which is a typical indication of the presence of fine grained magnetite (Fe_3O_4) [*Dunlop and Ozdemir*, 1997]. Narrow grain size distribution and relatively large magnetite crystals could be responsible for the sharp decrease of the signal at sample PL2o. The rest of the sites show more gentle convex shapes of the heating curves, suggesting wider grain size distribution of magnetite particles. The decrease of susceptibility after cooling back to room temperature is most probably due to oxidation of magnetite during heating. This process caused also the appearance of hematite component with T_N of 700°C for the samples PL2o and SZ1o. Secondary (laboratory induced) origin of hematite is assumed, taking into account the absence of any remanence acquisition in high dc fields during IRM acquisition experiment, shown in Figure 6. The shape of the heating curve for the dust sample from Burgas (B2o) suggests the presence of additional Tc of about 480°C, which can be attributed to titanomagnetite. This titanomagnetite phase is widely found in soils from Burgas region [*Jordanova and Jordanova*, 2010]. Similar to our data, magnetite as a carrier of the magnetic signal of atmospheric dust is reported in a number of recent studies [*Muxworthy et al.*, 2002, 2003; *Sagnotti et al.*, 2006; *Xia et al.*, 2008; *Elzinga et al.*, 2011]. The grain size of the magnetic fraction in indoor and outdoor dusts could be deduced from the hysteresis parameters, having proven the dominance of magnetite [*Dunlop*, 1986]. Hysteresis loops closed at fields up to 300 mT (Figure 7a) and the signal saturated are indicative for magnetically soft grains (e.g., magnetite) in accordance with the results from thermomagnetic analyses. Systematically lower remanent coercivities of outdoor dusts relative to indoor pair (Figure 7b) prove the concept that finer particles are settled inside the buildings as a result of gravitational differentiation. Moreover, significantly higher paramagnetic component in outdoor dusts (Figure 7c) points to a higher portion of paramagnetic minerals, deposited outdoors. A possible source of such particles is the soil dust component. A Day plot (Figure 7d) gives further evidence that the effective magnetic grain size of the magnetic fraction is pseudo-single domain. Deviation of the experimental data points from the mixing line of SD + MD grains [*Dunlop*, 2002] suggests that the magnetic fraction in the dust samples is not a bimodal mixture of coarse and fine grains. Rather, the data set except samples from Burgas (data points from the lower right corner of the PSD region) fits well to the mixing SP + PSD curve (ferrofluid 9.3 nm and 1–3 μm hydrothermal magnetites) from the same work [*Dunlop*, 2002], revealing possible 10–25% SP component in the settled dust. Comparison with the grain-size dependence of magnetic parameters for magnetite (M_{rs}/χ and B_{cr}), compiled by *Peters and Dekkers* [2003] also implies the predominance of 1–3 μm magnetite grains. Calculated M_{rs}/χ ratio for 10 indoor dusts gives mean value of $11.33 \pm 2.97 \times 10^3$ A/m, and value of $9.98 \pm 2.58 \times 10^3$ A/m for 16 outdoor dust samples, falling in the range of values of M_{rs}/χ typical for small PSD magnetite grains. This grain size inference is supported by the identified peak at (1.3–1.8))μm in the number concentration of mineral particles (Table 2). Predominance of the fine silt fraction ($d < 30$ μm) observed under light microscope in the studied samples (Figure 8) implies that urban indoor and outdoor dust contains fine grained particles. Systematically lower proportion of $d < 30$ μm in outdoor dusts as compared to indoor dusts (Figure 8) proves the general observation that settled dust indoor has smaller mean grain size than the outdoor dust.

[28] The presence of anthropogenic magnetic particles in the settled dusts is ascertained by the identified spherules (Figures 9a and 9d), which usually originate from combustion processes [*McLennan et al.*, 2000; *Kukier et al.*, 2003]. Smaller Fe-containing clusters of particles (Figure 9b) are most probably exhaust particles from diesel combustion vehicles. Atmospheric dust has also affected the pollen grains, which are characterized by dense cover of fine dust particles on their surfaces (Figure 9c). This adherence of fine particulate matter to the pollen grains is another factor, which increases the allergenic potential of pollens and makes them more aggressive to the immune system [*D'Amato et al.*, 2002, 2007].

4.3. Heavy Metal Content, PAHs and Magnetism

[29] Contamination of settled dust with hazardous substances is a well-known phenomenon, which is related to emissions from various sources such as vehicles, industrial production, coal and wood firing, etc. [*Menichini*, 1992; *Azimi et al.*, 2005]. The measured concentrations of the major toxic heavy metals in studied indoor and outdoor dusts (Table 2) indicate significant enhancement of As, Pb, Zn and Cu in all samples, compared with typical values for non-contaminated soils and major rock types [*Alloway*, 1995]. Based on the results from cluster

analysis, data for Burgas (samples B2o and B1o) were considered separately. We examined the possibility of having high HM content inherited from the soil derived and lithogenic component. Previous magnetic and geochemical studies of different soils from Burgas region [*Jordanova and Jordanova*, 2010] however, report significantly lower concentrations of the listed heavy metals in the soil cover, compared to the composition of the dust samples in the present investigation. Thus, lithogenic component as possible source of heavy metals in Bourgas settled dusts can be discarded. Another possible explanation for the very high regional concentrations of As and heavy metals is identified by moss monitoring of long-distance trans-boundary pollution from Turkey coming from two glass factories [*Coskun et al.*, 2009]. On the other hand, extremely high content of As is accompanied by very high Cu content in the sample B2o from Burgas, suggesting that this pollution may be caused by emissions from Cu-smelting industry in the region.

[30] Analyses on dust samples have been done for the summer months (June–August 2009), thus avoiding contribution from emissions of heating systems (coal and wood firing domestic and public installations) as one possible source of pollution. According to the analysis of principal components, several factors account for variability in the data set. Factor 1 with the highest loadings by Fe, Mn and χ explain 40.6% of the total variance and can be attributed to soil dust and re-suspended lithogenic component. The second factor, determining another major source of heavy metal pollution by As and Pb could be assigned to vehicle emissions [*Johansson et al.*, 2009]. The third factor with main loadings from Co and Cr may be attributed to industrial activities [*Alloway*, 1995]. The fourth factor accounts for 9% of the total variance with major contribution from Ni and Cu. The latter element is known to originate largely from brake wear [*Hulskotte et al.*, 2006; *Thorpe and Harrison*, 2008]. The calculated Tomlinson pollution index (PLI), giving an estimate of the total HM load indicates that most of the samples fall in the category of moderately polluted with PLI in the interval 2–3 [*Angulo*, 1996]. Plovdiv (P2o) and Burgas (B2o) outdoor dusts can be classified as moderately and highly polluted respectively. The latter two locations are at the closest distance to the roads (see Table 1), suggesting traffic as a main pollution source.

[31] Tomlinson pollution index (PLI) shows significant at $p < 0.05$ correlations with Pb, Zn, As and Ni, due to the predominance of these pollutants (Table 4). Mass specific magnetic susceptibility does not correlate significantly with PLI due to two major factors: i) data set is composed of samples from different regions, which have various lithogenic composition of the soil – derived dust component; ii) various pollution sources, whose emissions contain different magnetic fractions. As a consequence, magnetic susceptibility for distinct multiregional data set is not directly related to the degree of pollution.

[32] Polycyclic aromatic hydrocarbons (PAHs) are formed as a result of incomplete combustion (pyrolysis) or high temperature pyrolytic process during combustion of fossil fuels/organic materials, as well as in natural processes such as carbonization (pyrosynthesis), by-products of incineration of industrial and urban wastes, oil spills and vehicle exhausts. Motor vehicle emissions (especially diesel vehicles) make a considerable contribution to PAH concentration in air due to burning and incomplete combustion of diesel or gasoline. Most of the PAHs are highly toxic substances, playing important role for the human health [*Kameda et al.*, 2005; *Chen and Liao*, 2006; *Srogi*, 2007; *Maertens et al.*, 2008]. Although a limited number of samples were analyzed for PAH content (Table 3), it can be concluded that high molecular weight 5-ring PAHs (BbF, BkF, DahA) are the dominant compounds. These are reported as major emissions from diesel vehicles [*Marr et al.*, 1999]. Concentrations of some PAH marker compounds and their ratios can give indication about the impact of different sources of airborne compounds [*Guo et al.*, 2003; *Tobiszewski and Namiesnik*, 2012]. Table 5 provides the calculated values of diagnostic ratios for PAHs, such as R_{178} = Ant/(Ant + Flu); R_{202} = Flu/(Flu + Pyr); R_{228} = BaA/(BaA + Chr), and R_{276} = IcdP/(IcdP + BghiP) [*Yunker et al.*, 2002]. Very similar values are obtained for the ratio R_{202}:<0.5 for the samples B2o, R1o, PL2o, S3o and SZ1o, indicating that Ant and Flu originate from combustion in diesel cars; while for the other samples $R_{202} > 0.5$, suggesting that these PAHs are produced during vegetation and coal burning [*Yunker et al.*, 2002]. The mean level of ΣPAHs in this study (0.57–8.3 mg/kg) is close to those in Guangzhou, China (0.84–12.3) mg/kg [*Wang et al.*, 2011], Greater Cairo, Egypt (0.045–2.61 mg/kg) and relatively higher than those in the United Kingdom (0.002 mg/kg), Norway (0.0069 mg/kg), Canada (0.0011 mg/kg) and Australia (0.0033 mg/kg) [*Hassanien and Abdel-Latif*, 2008, and references therein].

[33] Link between magnetic parameters of urban dust and its PAH content is reported in several

studies, which found a linear relationship between PAH content and M_{rs} [*Lehndorff and Schwark*, 2004; *Halsall et al.*, 2008; *Jordanova et al.*, 2010]. In the present study, we found dependency between total PAH content and grain-size sensitive magnetic parameters, e.g., coercivity of remanence (B_{cr}) and the ratio M_{rs}/χ (Figure 11). It indicates that higher PAH content is linked to dust samples with smaller effective magnetic grain sizes of the magnetic fraction (magnetite). This relationship could be explained in two alternative ways: i) either increased content of PAHs is due to an increase in surface adsorption caused by higher surface/volume ratio with decrease of particle size; or ii) combustion processes responsible for PAH emissions vary in a way that higher amount of PAHs is linked to correspondingly smaller grains of the accompanying magnetic fraction. Affinity of PAHs for sorption onto inorganic particles has been studied by *Fang et al.* [2008]. They show that surface adsorption mechanism is the main sorption process of phenanthrene on zero valent iron, copper and silicon dioxide engineered nanoparticles.

4.4. Magnetic Properties of Settled Dust and Health Indicators

[34] Extensive number of publications have shown that the concentration dependent magnetic parameters such as magnetic susceptibility (χ) can be used as a proxy for the pollution degree (for reviews see *Petrovsky and Elwood* [1999] and *Evans and Heller* [2003]). Only one publication up to our knowledge deals with interdisciplinary research directed toward combined use of magnetic studies and health data. In this work, *Morris et al.* [1995] found out significant correlation between mutagenicity of the organic compounds of dust from filters, and the values of magnetic susceptibility of the mineral fraction. In this specific example, magnetic susceptibility of dust filters is directly compared to mutagenicity potency, as far as the study area has single pollution source and uniform background magnetic signal from the local lithogenic dust sources.

[35] General question arise before any attempts to correlate magnetic and health data: what is the direct (or indirect) link between the two parameters? Are magnetic compounds toxic and dangerous for human health? Literature review shows that toxicological and epidemiological studies are reported for nanosized compounds, which are often used in drug delivery as well as for contrasting agents [*Weinstein et al.*, 2010]. Genotoxicity of 1–3 μm magnetite particles and subway particles rich in magnetite was examined by *Karlsson et al.* [2008], who found much higher DNA damage to human cells by subway particles than that of pure magnetite. *Singh et al.* [2010] and *Mahmoudi et al.* [2011] reviewed publications on cellular toxicity, DNA damage and oxidative stress caused by superparamagnetic iron oxide nanoparticles, coated or uncoated by various substances used in biomedical applications. Cytotoxicity and genotoxicity of size-fractionated magnetite was studied by *Konczol et al.* [2011], revealing that the major genotoxicity effect of magnetite particles on human alveolar cells is production of reactive oxygen species (ROS). Furthermore, they demonstrate that magnetite particles induce concentration-dependent DNA damage. A slight size dependency is observed, as the larger particles induced less genotoxicity. Extensive study on size dependence of toxicity of metal oxide particles by *Karlsson et al.* [2009] found that there is no general trend for nanosized particles to be more toxic than micrometer-sized, but rather it depends on the mineral type. Based on this information we can assume that the magnetic fraction in the urban dust can also play role in generation of negative effects on human health.

[36] Assuming initially that toxicological effects of iron oxides are simply related to concentration changes, we examine the existence of relationships between mass-specific magnetic susceptibility (χ) of both indoor and outdoor dusts, and mortality rates caused by respiratory and cardiovascular diseases (Figure 12). The absence of such dependence is most probably related to different contribution of various sources of magnetic particles in the sampled dust. To take it into account, we examined the possibility of "normalization" of mass specific susceptibility to a parameter, which would represent the regional urban background. Magnetic susceptibility of natural soils, spread in the surroundings of the corresponding city cannot be used as a "background" signal for several reasons: i) in some places wide variety of soil types with contrasting magnetic susceptibilities are present. For example in Sofia valley, soil types range from weakly magnetic Vertisols up to strongly magnetic Cambisols; ii) there are in general very different proportions of soil-derived material with respect to the anthropogenic fraction in different dust samples. Therefore, normalizing to a value, corresponding to 100% topsoil, will not help to discriminate the two contributions. This leads us to use another approach. We calculate the ratio of indoor to outdoor susceptibilities (χ_{indoor}/

$\chi_{outdoor}$). This ratio can be considered as analogous to the indoor/outdoor (I/O) ratios frequently reported for the PM concentrations and various chemical elements. Different values of the I/O parameter are reported for various grain sizes and different chemical elements [*Jones et al.*, 2000; *Chen and Zhao*, 2011]. In the absence of indoor sources, I/O ratio is less or equal to 1. Concerning the origin of magnetic susceptibility signal of settled dust, similar considerations can be applied. The magnetic susceptibility of outdoor dust reflects the mixed contribution of: i) soil-derived strongly magnetic dust particles and ii) anthropogenic (industrial, traffic-related, fossil-fuel etc.) particles. Indoor dust in the present study has mainly an ambient origin, i.e., it contains magnetic particles of similar origin, but with grain sizes selectively oriented toward finer sizes. This fining of infiltrated and penetrated magnetic fraction is due to the fact that coarse particles penetrate with more difficulty indoors due to gravitational differentiation. This implies that most of the coarse dust particles will be settled outside, while only finer grained particles could penetrate indoors. Close proximity of the sampled locations, which correspond to an outdoor and indoor sampling point was used to assure that there will be no significant differences in the main dust source. In case of equal conditions for penetration, infiltration and re-suspension of dust particles, the amount of ambient (outdoor) particles indoor will depend on the size distribution and amount of anthropogenically derived magnetic particles. Thus, high values of the ratio ($\chi_{indoor}/\chi_{outdoor}$) will be obtained if larger quantities of outdoor particles penetrate indoors, and vice versa. Combustion (both industrial and traffic-related) is the primary source of most carcinogenic and toxicogenic particulates in ambient air, and it generates particles in the fine grained range (PM10 in general). Consequently, the amount of combustion-originating magnetic particles which penetrate indoors will be mostly responsible for χ_{indoor}. In favor of differential infiltration behavior of dust particles with different origin are the results presented by *Meng et al.* [2007], who showed that infiltration factors for PM2.5 originating from primary combustion, secondary formation and mechanical formation differ significantly, being much higher for the first two groups of particles. The obtained range of variations of the ratio $\chi_{indoor}/\chi_{outdoor}$ may be compared to the widely studied PM_{10} mass indoor/outdoor (I/O) ratio [*Thatcher and Layton*, 1995; *Jones et al.*, 2000; *Liao et al.*, 2003, 2004]. This similarity suggests that magnetic fraction in indoor and outdoor dusts obeys the same behavior as the major mineral dust components, contributing to the amount of PM.

[37] Comparison between mean annual values of $\chi_{indoor}/\chi_{outdoor}$ per city with the corresponding data on mortality caused by respiratory and cardiovascular diseases (Figure 13) reveals the existence of a linear correlation between the ratio $\chi_{indoor}/\chi_{outdoor}$ and the number of people dying as a result of cardiovascular diseases. The obtained correlation coefficient R^2 of 0.82 at $p < 0.05$ significance level refers to the classical calculation without accounting for the error bars on χ-ratio. A t-test is applied in order to test the significance of the regression, i.e., hypothesis that the slope of the regression equation (b_2) is equal to zero. Rejection of the null hypothesis has been obtained, suggesting that the fitted regression model is of value in explaining variations in the observations. Confidence Intervals on Regression Coefficients (intercept b_1 and slope b_2) has been determined as well [*Sen and Srivastava*, 1990; *Montgomery et al.*, 2001]. Figure 14a shows the estimated confidence area determined by b_1 and b_2, which is significantly different from the line of zero slope, thus proving the significance of the regression. Equations used for statistical tests on the significance of the linear regression are given in the auxiliary material.[1] Taking into account the experimental errors in χ-ratio, plot of the highest posterior density within the 95% envelope (Figure 14b) shows that there is still significant relationship between magnetic ratio and cardiovascular mortality.

[38] The obtained correlation could be tentatively explained by the following considerations. The ratio $\chi_{indoor}/\chi_{outdoor}$ primarily depends on the amount of outdoor magnetic particles, which were able to penetrate indoors. These are, as discussed above, enriched in finer material of anthropogenic origin. The greater number of particles of this origin penetrating indoors, the higher will be the risk for PM-related health problems. Thus, higher values of $\chi_{indoor}/\chi_{outdoor}$ signify an increased anthropogenic pollution level indoors. Due to the long time spent by people indoors [*Klepeis et al.*, 2001], proportional increases in mortality caused by cardiovascular diseases with increased values of $\chi_{indoor}/\chi_{outdoor}$ should be expected. Now an important issue is why and how increases in atmospheric pollution are more relevant to mortality caused by cardiovascular diseases (myocardial infarction, heart failure, and fatal arrhythmias) and not so significant in respiratory diseases. The traditional view that the lungs are most affected by air pollution is not supported by the epidemiological evidence during the last 15 years [*Johnson*, 2004]. *Pope*

[1] Auxiliary materials are available in the HTML. doi:10.1029/2012GC004160.

et al. [2004, p. 71] also report that "fine particulate air pollution is a risk factor for cause-specific cardiovascular disease mortality via mechanisms that likely include pulmonary and systemic inflammation, accelerated atherosclerosis, and altered cardiac autonomic function. Although smoking is a much larger risk factor for cardiovascular disease mortality, exposure to fine PM imposes additional effects that seem to be at least additive to if not synergistic with smoking." A recent review [*de Kok et al.*, 2006] shows that toxicity of ambient and traffic-related PM is not always proportional to the intensity of the traffic but rather is source-dependent. This implies that our approach in using close pairs of indoor – outdoor sites for estimation of health impact of urban dust is highly relevant.

[39] The obtained scatter in the plot of the ratio $\chi_{indoor}/\chi_{outdoor}$ versus mortality caused by respiratory diseases (Figure 13a) could be due to the fact that respiratory tract is much more influenced by tobacco smoke, the latter being among the primary causes of lethal effects for vulnerable population [*Hecht*, 1999]. Data points which deviate the most from tentative linear dependence are data for Burgas (2009 and 2010), Russe and Plovdiv – 2010 data.

5. Envisaged Drawbacks, Advantages and Future Perspectives of the Application of Magnetic Proxies in Health Studies

[40] Magnetic susceptibility is one fundamental and easily measurable parameter in environmental studies, reflecting the presence of strongly magnetic particles. Its high sensitivity toward ferrimagnetic minerals allows detailed records of changing source, sedimentation rate and grain size distribution of dust material to be obtained. In this respect, unfavorable conditions for application of magnetic monitoring would appear if dust loading is interrupted, polluted from metallic particles not related to the general pattern of atmospheric emissions, etc. Important environmental parameters, which influence significantly magnetic measurements, are microclimatic conditions, e.g., local wind speed; precipitation; humidity. In order to reach suitable representative estimate of magnetic behavior of the settled dust, one needs to find a quiet microenvironment sheltered from rain/snow, which should further represent an inaccessible place to prevent unwanted human disturbances as well. Along with these requirements, sampling places should be chosen in view of the distribution of point and diffuse pollution sources. All these considerations make sampling design and strategy very important for successful implementation of environmental magnetic proxy estimates.

[41] A challenging topic in further research in this direction would be high-density mapping (or monitoring) the variations in the ratio $\chi_{indoor}/\chi_{outdoor}$ of spatially distributed sampling points within a town, coupled with detailed medical records of admissions with acute respiratory and cardiovascular problems, monthly data for mortality rates and air quality data (PM10 concentrations, NOx, SOx, etc.). Establishing the mean value for the magnetic parameter $\chi_{indoor}/\chi_{outdoor}$ for the whole city, hot spots of high values would indicate the highest risk for health problems caused by atmospheric pollution. Furthermore, magnetic inventory of indoor pollution sources would be the second challenge, which will allow to check the applicability of the proposed new approach in case of significant indoor pollution sources.

6. Conclusions

[42] 1. Mass-specific magnetic susceptibility of outdoor settled dusts from six cities in Bulgaria show systematically higher values than susceptibility of the corresponding indoor locations. This general property is accompanied by higher dust loading rates for most outdoor sites except the ones, exposed to strong local wind circulation. The absence of seasonal variations and correspondence with PM10 concentrations indicate that the sampled settled dusts most probably are influenced by diffuse pollution sources such as traffic.

[43] 2. The anthropogenic magnetic fraction in dust samples is represented by magnetite. SEM observations prove that it contains large portion of spherules from traffic – related exhaust emissions and industrial combustion processes. Dust samples from the city of Burgas have strongly magnetic soil-derived component, presented by titanomagnetite(s) with Tc of 500°C.

[44] 3. Hysteresis measurements suggest that the magnetic fraction in the studied dust samples is in pseudo-single-domain state. Indoor dusts are generally characterized by higher coercivity (B_{cr}) compared to their outdoor counterparts, which proves that the main source of the indoor dusts is the outdoor material. Due to the common gravitational differentiation, smaller dust particles can penetrate indoor.

[45] 4. Statistical analysis of the data on heavy metal content and magnetic susceptibility suggest the presence of several sources of pollution. Factor analysis classifies mass specific susceptibility in a factor with highest loadings from Fe and Mn, explaining 40.5% of the total variance. It suggests crustal (soil derived) or industrial (Mn-producing) source. The second factor explains 21% of the total variance and has the highest loadings from As, Pb and PLI index, indicating traffic-related sources. The third factor with an eigenvalue higher than 1, is determined by Co and Cr, probably confirming the role of industrial pollution, which accounts for 13.6% of the total variance.

[46] 5. Total PAH content of the outdoor dusts show positive correlation with the grain size dependent magnetic parameters B_{cr} and M_{rs}/χ, suggesting either surface adsorption of PAHs onto iron oxide particles with increasing surface/volume ratio, or simultaneous increase in PAH concentration with decreased size of the magnetic fraction accompanying PAH emissions.

[47] 6. The mean ratio $\chi_{indoor}/\chi_{outdoor}$ for each city shows significant correlation with mortality caused by cardiovascular diseases. It allows wide application of magnetic methods in health and epidemiological studies.

Acknowledgments

[48] This study is carried out in the frame of the project DO 02-193/2008 "Geophysical investigations of the environmental pollution level and its effect on human health in urban areas" funded by the Bulgarian National Science Fund. The authors highly acknowledge English language corrections kindly done by C. Batt (Univ. Bradford, UK). Special thanks are due to the local public authorities, who provided access to the indoor sites.

References

Abdul-Razzaq, W., and M. Gautam (2001), Discovery of magnetite in the exhausted material from the diesel engine, *Appl. Phys. Lett.*, *78*, 2018–2019.

Aimar, S. B., M. J. Mendez, R. Funk, E. Daniel, and D. E. Buschiazzo (2012), Soil properties related to potential particulate matter emissions (PM10) of sandy soils, *Aeolian Res.*, *3*, 437–443.

Alloway, B. J. (Ed.) (1995), *Heavy Metals in Soils*, 368 pp., Blackie Acad. and Prof., Glasgow, U. K.

Angulo, E. (1996), The Tomlinson Pollution Load Index applied to heavy metal, 'Mussel-Watch' data: A useful index to assess coastal pollution, *Sci. Total Environ.*, *187*(1), 19–56.

Azimi, S., V. Rocher, M. Muller, R. Moilleron, and D. Thevenot (2005), Sources, distribution and variability of hydrocarbons and metals in atmospheric deposition in an urban area (Paris, France), *Sci. Total Environ.*, *337*, 223–239.

Brunekreef, B., and B. Forsberg (2005), Epidemiological evidence of effects of coarse airborne particles on health, *Eur. Respir. J.*, *26*, 309–318.

Burnett, R. T., S. Cakmak, J. R. Brook, and D. Krewski (1997), The role of particulate size and chemistry in the association between summertime ambient air pollution and hospitalization for cardiorespiratory diseases, *Environ. Health Perspect.*, *105*, 614–620.

Chen, C., and B. Zhao (2011), Review of relationship between indoor and outdoor particles: I/O ratio, infiltration factor and penetration factor, *Atmos. Environ.*, *45*, 275–288.

Chen, S. C., and C. M. Liao (2006), Health risk assessment on human exposed to environmental polycyclic aromatic hydrocarbons pollution sources, *Sci. Total Environ.*, *366*, 112–123.

Coskun, M., L. Yurukova, A. Çayir, M. Coskun, and G. Gecheva (2009), Cross-border response of mosses to heavy metal atmospheric deposition in southeastern Bulgaria and European Turkey, *Environ. Monit. Assess.*, *157*, 529–537.

D'Amato, G., G. Liccardi, M. D'Amato, and M. Cazzola (2002), Outdoor air pollution, climatic changes and allergic bronchial asthma, *Eur. Respir. J.*, *20*, 763–776.

D'Amato, G., L. Cecchi, S. Bonini, C. Nunes, I. Annesi-Maesano, H. Behrendt, G. Liccardi, T. Popov, and P. van Cauwenberge (2007), Allergenic pollen and pollen allergy in Europe, *Allergy*, *62*, 976–990.

Davidson, C. I., R. F. Phalen, and P. A. Solomon (2005), Airborne particulate matter and human health: A review, *Aerosol Sci. Technol.*, *39*(8), 737–749.

Day, R., M. Fuller, and V. A. Schmidt (1977), Hysteresis properties of titanomagnetites: Grain size and compositional dependence, *Phys. Earth Planet. Inter.*, *13*, 260–267.

Dearing, J. (1999), Magnetic susceptibility, in *Environmental Magnetism: A Practical Guide*, *Tech. Guide*, vol. 6, edited by J. Walden, F. Oldfield, and J. P. Smith, pp. 35–62, Quat. Res. Assoc., London.

de Kok, T., H. A. L. Driece, J. G. F. Hogervorst, and J. J. Briede (2006), Toxicological assessment of ambient and traffic-related particulate matter: A review of recent studies, *Mutat. Res.*, *613*, 103–122.

Donaldson, K., et al. (2005), Combustion-derived nanoparticles: A review of their toxicology following inhalation exposure, *Part. Fibre Toxicol.*, *2*, 10.

Dunlop, D. (1986), Hysteresis properties of magnetite and their dependence on particle size: A test of pseudo-single-domain remanence models, *J. Geophys. Res.*, *91*(B9), 9569–9584.

Dunlop, D. (2002), Theory and application of the Day plot (Mrs/Ms versus Hcr/Hc): 1. Theoretical curves and tests using titanomagnetite data, *J. Geophys. Res.*, *107*(B3), 2056, doi:10.1029/2001JB000486.

Dunlop, D., and O. Ozdemir (1997), *Rock Magnetism. Fundamentals and Frontiers*, edited by D. Edwards, Cambridge Univ. Press, Cambridge, U. K.

Elzinga, E. J., Y. Gao, J. P. Fitts, and R. Tappero (2011), Iron speciation in urban dust, *Atmos. Environ.*, *45*, 4528–4532.

Evans, M., and F. Heller (2003), *Environmental Magnetism. Principles and Applications of Enviromagnetics*, Academic, San Diego, Calif.

Fang, J., X. Shan, B. Wen, J. Lin, X. Lu, X. Liu, and G. Owens (2008), Sorption and desorption of phenanthrene onto iron, copper, and silicon dioxide nanoparticles, *Langmuir*, *24*, 10,929–10,935.

Fisher, B., and J. Macqueen (1981), A theoretical model for particulate transport from an elevated source in the atmosphere, *IMA J. Appl. Math.*, *27*(3), 359–371.

Foret, G., G. Bergametti, F. Dulac, and L. Menut (2006), An optimized particle size bin scheme for modeling mineral dust aerosol, *J. Geophys. Res.*, *111*, D17310, doi:10.1029/2005JD006797.

Goddu, S. R., E. Appel, D. Jordanova, and F. Wehland (2004), Magnetic properties of road dust from Visakhapatnam (India)—Relationship to industrial pollution and road traffic, *Phys. Chem. Earth*, *29*, 985–995.

Gomes, S., M. Francois, M. Abdelmoula, P. Refait, C. Pellissier, and O. Evrard (1999), Characterization of magnetite in silico-aluminous fly ash by SEM, TEM, XRD, magnetic susceptibility and Mössbauer spectroscopy, *Cement Concr. Res.*, *29*, 1705–1711.

Goossens, D., and B. Buck (2011), Gross erosion, net erosion and gross deposition of dust by wind: Field data from 17 desert surfaces, *Earth Surf. Processes Landforms*, *36*, 610–623.

Guo, H., S. C. Lee, K. F. Ho, X. M. Wang, and S. C. Zou (2003), Particle-associated polycyclic aromatic hydrocarbons in urban air of Hong Kong, *Atmos. Environ.*, *37*, 5307–5317.

Halsall, C. J., B. A. Maher, V. V. Karloukovski, P. Shah, and S. J. Watkins (2008), A novel approach to investigating indoor/outdoor pollution links: Combined magnetic and PAH measurements, *Atmos. Environ.*, *42*, 8902–8909.

Hanesch, M., R. Scholger, and D. Rey (2003), Mapping dust distribution around an industrial site by measuring magnetic parameters of tree leaves, *Atmos. Environ.*, *37*, 5125–5133.

Hassanien, M. A., and N. M. Abdel-Latif (2008), Polycyclic aromatic hydrocarbons in road dust over greater Cairo, Egypt, *J. Hazard. Mater.*, *151*, 247–254.

Hecht, S. (1999), Tobacco smoke carcinogens and lung cancer—Review, *J. Natl. Cancer Inst.*, *91*(14), 1194–1210.

Hoffmann, V., M. Knab, and E. Appel (1999), Magnetic susceptibility mapping of roadside pollution, *J. Geochem. Explor.*, *66*(1–2), 313–326.

Hulskotte, J. H. J., M. Schaap, and A. J. H. Visschedijk (2006), Brake wear from vehicles as an important source of diffuse copper pollution, paper presented at 10th International Specialised Conference on Diffuse Pollution and Sustainable Basin Management, Istanbul Teknik Univ., Istanbul, Turkey, 18–22 Sept.

Johansson, C., M. Norman, and L. Burman (2009), Road traffic emission factors for heavy metals, *Atmos. Environ.*, *43*, 4681–4688.

Johnson, R. L., Jr. (2004), Relative effects of air pollution on lungs and heart, *Circulation*, *109*, 5–7.

Jones, N. C., C. A. Thornton, D. Mark, and R. M. Harrison (2000), Indoor/outdoor relationships of particulate matter in domestic homes with roadside, urban and rural locations, *Atmos. Environ.*, *34*, 2603–2612.

Jordanova, N., and D. Jordanova (2010), Magnetic methods for delineation of heavy metal pollution in Burgas region, paper presented at 10th International Multidisciplinary Scientific GeoConference SGEM, Bulg. Acad. of Sci., Albena, Bulgaria.

Jordanova, N. V., D. V. Jordanova, L. Veneva, K. Yorova, and E. Petrovsky (2003), Magnetic response of soils and vegetation to heavy metal pollution—A case study, *Environ. Sci. Technol.*, *37*, 4417–4424.

Jordanova, D., P. Petrosv, V. Hoffmann, T. Gocht, C. Panaiotu, T. Tsacheva, and N. Jordanova (2010), Magnetic signature of different vegetation species in polluted environment, *Stud. Geophys. Geod.*, *54*(3), 417–442.

Kameda, Y., J. Shirai, T. Komai, J. Nakanishi, and S. Masunaga (2005), Atmospheric polycyclic aromatic hydrocarbons: Size distribution, estimation of their risk and their depositions to the human respiratory tract, *Sci. Total Environ.*, *340*, 71–80.

Karlsson, H. L., Å. Holgersson, and L. Möller (2008), Mechanisms related to the genotoxicity of particles in the subway and from other sources, *Chem. Res. Toxicol.*, *21*, 726–731.

Karlsson, H. L., J. Gustafsson, P. Cronholm, and L. Möller (2009), Size-dependent toxicity of metal oxide particles—A comparison between nano- and micrometer size, *Toxicol. Lett.*, *188*, 112–118.

Kim, W., S. J. Doh, Y. H. Park, and S. T. Yun (2007), Two-year magnetic monitoring in conjunction with geochemical and electronmicroscopic data of roadside dust in Seoul, Korea, *Atmos. Environ.*, *41*, 7627–7641.

Kim, W., S. J. Doh, and Y. Yu (2009), Anthropogenic contribution of magnetic particulates in urban roadside dust, *Atmos. Environ.*, *43*, 3137–3144.

Klepeis, N. E., W. C. Nelson, W. R. Ott, J. P. Robinson, A. M. Tsang, P. Switzer, J. V. Behar, S. C. Hern, and W. H. Engelmann (2001), The National Human Activity Pattern Survey (NHAPS): A resource for assessing exposure to environmental pollutants, *J. Exposure Anal. Environ. Epidemiol.*, *11*, 231–252.

Konczol, M., S. Ebeling, E. Goldenberg, F. Treude, R. Gminski, R. Giere, B. Grobety, B. Rothen-Rutishauser, I. Merfort, and V. Mersch-Sundermann (2011), Cytotoxicity and genotoxicity of size-fractionated iron oxide (magnetite) in A549 human lung epithelial cells: Role of ROS, JNK, and NF-kB, *Chem. Res. Toxicol.*, *24*, 1460–1475.

Kukier, U., C. Ishak, M. Sumner, and W. Miller (2003), Composition and element solubility of magnetic and non-magnetic fly ash fractions, *Environ. Pollut.*, *123*, 255–266.

Lanos, P. (2004), Bayesian inference of calibration curves: Application to archaeomagnetism, in *Tools for Constructing Chronologies: Crossing Disciplinary Boundaries*, vol. 177, edited by C. Buck and A. Millard, pp. 43–82, Springer, London.

Lehndorff, E., and L. Schwark (2004), Biomonitoring of air quality in the Cologne Conurbation using pine needles as a passive sampler. Part II: Polycyclic aromatic hydrocarbons (PAH), *Atmos. Environ.*, *38*(23), 3793–3808.

Lehndorff, E., M. Urbat, and L. Schwark (2006), Accumulation histories of magnetic particles on pine needles as function of air quality, *Atmos. Environ.*, *40*(36), 7082–7096.

Liao, C. M., J. W. Chen, and S. J. Huang (2003), Size-dependent PM10 indoor/outdoor/personal relationships for a wind-induced naturally ventilated airspace, *Atmos. Environ.*, *37*, 3065–3075.

Liao, C. M., S. J. Huang, and H. Yu (2004), Size-dependent particulate matter indoor/outdoor relationships for a wind-induced naturally ventilated airspace, *Build. Environ.*, *39*, 411–420.

Lippmann, M. (2011), Particulate matter (PM) air pollution and health: Regulatory and policy implications, *Air Qual. Atmos. Health*, *5*, 1–5.

Lippmann, M., K. Ito, A. Nadas, and R. T. Burnett (2003), Association of particulate matter components with daily mortality and morbidity in urban populations, *Res. Rep.*, *95*, pp. 5–82, Health Eff. Inst., Boston, Mass.

Liu, Y.-J., and R. M. Harrison (2011), Properties of coarse particles in the atmosphere of the United Kingdom, *Atmos. Environ.*, *45*, 3267–3276.

Maertens, R. M., J. Bailey, and P. A. White (2004), The mutagenic hazards of settled house dust: A review, *Mutat. Res.*, *567*, 401–425.

Maertens, R. M., X. F. Yang, J. P. Zhu, R. W. Gagne, G. R. Douglas, and P. A. White (2008), Mutagenic and carcinogenic hazards of settled house dust I: Polycyclic aromatic

hydrocarbon content and excess lifetime cancer risk from preschool exposure, *Environ. Sci. Technol.*, *42*, 1747–1753.
Maher, B. A., C. Moore, and J. Matzka (2008), Spatial variation in vehicle-derived metal pollution identified by magnetic and elemental analysis of roadside tree leaves, *Atmos. Environ.*, *42*, 364–373.
Mahmoudi, M., K. Azadmanesh, M. A. Shokrgozar, W. S. Journeay, and S. Laurent (2011), Effect of nanoparticles on the cell life cycle, *Chem. Rev.*, *111*, 3407–3432.
Marr, L. C., T. W. Kirchstetter, R. A. Harley, A. H. Miguel, S. V. Hering, and S. K. Hammond (1999), Characterization of polycyclic aromatic hydrocarbons in motor vehicles fuel and exhaust emissions, *Environ. Sci. Technol.*, *33*, 3091–3099.
Marticorena, B., and G. Bergametti (1995), Modeling the atmospheric dust cycle: 1. Design of a soil-derived dust emission scheme, *J. Geophys. Res.*, *100*(D8), 16,415–16,430.
Matzka, J., and B. A. Maher (1999), Magnetic biomonitoring of roadside tree leaves: Identification of spatial and temporal variations in vehicle-derived particulates, *Atmos. Environ.*, *33*, 4565–4569.
McLennan, A. R., G. W. Bryant, B. R. Stanmore, and T. F. Wall (2000), Ash formation mechanism during pf combustion in reducing conditions, *Energy Fuels*, *14*, 150–159.
Meng, Q. Y., B. J. Turpin, J. H. Lee, A. Polidori, C. P. Weisel, M. Morandi, S. Colome, J. Zhang, T. Stock, and A. Winer (2007), How does infiltration behavior modify the composition of ambient PM2.5 in indoor spaces? An analysis of RIOPA data, *Environ. Sci. Technol.*, *41*, 7315–7321.
Menichini, E. (1992), Urban air pollution by polycyclic aromatic hydrocarbons: Levels and sources of variability, *Sci. Total Environ.*, *116*(1–2), 109–135.
Mitchell, R., and B. A. Maher (2009), Evaluation and application of biomagnetic monitoring of traffic-derived particulate pollution, *Atmos. Environ.*, *43*, 2095–2103.
Mitchell, R., B. A. Maher, and R. Kinnersley (2010), Rates of particulate pollution deposition onto leaf surfaces: Temporal and inter-species magnetic analyses, *Environ. Pollut.*, *158*, 1472–1478.
Montgomery, D. C., E. A. Peck, and G. G. Vining (2001), *Introduction to Linear Regression Analysis*, 3rd ed., John Wiley, New York.
Morawska, L., and T. Salthammer (2003), Fundamentals of indoor particles and settled dust, in *Indoor Environment: Airborne Particles and Settled Dust*, edited by L. Morawska and T. Salthammer, pp. 3–46, John Wiley, Weinheim, Germany.
Morawska, L., Z. Ristovski, E. R. Jayaratne, D. U. Keogh, and X. Ling (2008), Ambient nano and ultrafine particles from motor vehicle emissions: Characteristics, ambient processing and implications on human exposure—Review, *Atmos. Environ.*, *42*, 8113–8138.
Morris, W. A., J. K. Versteeg, D. W. Bryant, A. E. Legzdins, B. E. McCarry, and B. H. Marvin (1995), Preliminary comparisons between mutagenicity and magnetic susceptibility of respirable airborne particulate matter, *Atmos. Environ.*, *29*(23), 3441–3450.
Muxworthy, A. R., J. Matzka, and N. Petersen (2001), Comparison of magnetic parameters of urban atmospheric particulate matter with pollution and meteorological data, *Atmos. Environ.*, *35*, 4379–4386.
Muxworthy, A. R., E. Schmidbauer, and N. Petersen (2002), Magnetic properties and Mössbauer spectra of urban atmospheric particulate matter: A case study from Munich, Germany, *Geophys. J. Int.*, *150*, 558–570.
Muxworthy, A. R., J. Matzka, A. F. Davila, and N. Petersen (2003), Magnetic signature of daily sampled urban atmospheric particles, *Atmos. Environ.*, *37*, 4163–4169.
Peters, C., and M. J. Dekkers (2003), Selected room temperature magnetic parameters as a function of mineralogy, concentration and grain size, *Phys. Chem. Earth*, *28*, 659–667.
Petrovsky, E., and B. Elwood (1999), Magnetic monitoring of air-, land- and water pollution, in *Quaternary Climates, Environments and Magnetism*, edited by B. Maher and R. Thompson, pp. 279–322, Cambridge Univ. Press, Cambridge, U. K.
Pope, A., et al. (1995), Particulate air pollution as a predictor of mortality in a prospective study of U.S. adults, *Am. J. Respir. Crit. Care Med.*, *151*, 669–674.
Pope, C. A., III, R. T. Burnett, M. J. Thun, E. E. Calle, D. Krewski, K. Ito, and G. D. Thurston (2002), Lung cancer, cardiopulmonary mortality, and long-term exposure to fine particulate air pollution, *JAMA J. Am. Med. Assoc.*, *287*(9), 1132–1141.
Pope, C. A., III, R. T. Burnett, G. D. Thurston, M. J. Thun, E. E. Calle, D. Krewski, and J. J. Godleski (2004), Cardiovascular mortality and long-term exposure to particulate air pollution. Epidemiological evidence of general pathophysiological pathways of disease, *Circulation*, *109*, 71–77.
Sagnotti, L., P. Macrı, R. Egli, and M. Mondino (2006), Magnetic properties of atmospheric particulate matter from automatic air sampler stations in Latium (Italy): Toward a definition of magnetic fingerprints for natural and anthropogenic PM10 sources, *J. Geophys. Res.*, *111*, B12S22, doi:10.1029/2006JB004508.
Sagnotti, L., J. Taddeucci, A. Winkler, and A. Cavallo (2009), Compositional, morphological, and hysteresis characterization of magnetic airborne particulate matter in Rome, Italy, *Geochem. Geophys. Geosyst.*, *10*, Q08Z06, doi:10.1029/2009GC002563.
Saragnese, F., L. Lanci, and R. Lanza (2011), Nanometric-sized atmospheric particulate studied by magnetic analyses, *Atmos. Environ.*, *45*, 450–459.
Sen, A., and M. Srivastava (1990), *Regression Analysis: Theory, Methods, and Applications*, Springer, New York.
Singh, N., G. Jenkins, R. Asadi, and S. H. Doak (2010), Potential toxicity of superparamagnetic iron oxide nanoparticles (SPION), *Nano Rev.*, *1*, 5358, doi:10.3402/nano.v1i0.5358.
Spassov, S., R. Egli, F. Heller, D. K. Nourgaliev, and J. Hannam (2004), Magnetic quantification of urban pollution sources in atmospheric particulate matter, *Geophys. J. Int.*, *159*, 555–564.
Srogi, K. (2007), Monitoring of environmental exposure to polycyclic aromatic hydrocarbons: A review, *Environ. Chem. Lett.*, *5*, 169–195.
Szönyi, M., L. Sagnotti, and A. M. Hirt (2008), A refined biomonitoring study of airborne particulate matter pollution in Rome, with magnetic measurements on Quercus Ilex tree leaves, *Geophys. J. Int.*, *173*, 127–141.
Thatcher, T. L., and D. W. Layton (1995), Deposition, resuspension and penetration of particles within a residence, *Atmos. Environ.*, *29*, 1487–1497.
Thorpe, A., and R. M. Harrison (2008), Sources and properties of non-exhaust particulate matter from road traffic: A review, *Sci. Total Environ.*, *400*, 270–282.
Tobiszewski, M., and J. Namiesnik (2012), PAH diagnostic ratios for the identification of pollution emission sources, *Environ. Pollut.*, *162*, 110–119.
Wang, W., M. Huang, Y. Kang, H. Wang, A. O. W. Leung, K. C. Cheung, and M. Wong (2011), Polycyclic aromatic hydrocarbons (PAHs) in urban surface dust of Guangzhou,

China: Status, sources and human health risk assessment, *Sci. Total Environ.*, *409*, 4519–4527.

Weinstein, J. S., C. G. Varallyay, E. Dosa, S. Gahramanov, B. Hamilton, W. D. Rooney, L. L. Muldoon, and E. A. Neuwelt (2010), Superparamagnetic iron oxide nanoparticles: Diagnostic magnetic resonance imaging and potential therapeutic applications in neuro oncology and central nervous system inflammatory pathologies, a review, *J. Cereb. Blood Flow Metab.*, *30*(1), 15–35.

World Health Organization (2006), Health risks of particulate matter from long-range transboundary air pollution, Eur. Cent. for Environ. and Health, Bonn, Germany.

Xia, D. S., F. H. Chen, J. Bloemendal, X. M. Liu, Y. Yu, and L. P. Yang (2008), Magnetic properties of urban dustfall in Lanzhou, China, and its environmental implications, *Atmos. Environ.*, *42*, 2198–2207.

Yang, T., Q. Liu, H. Li, Q. Zeng, and L. Chan (2010), Anthropogenic magnetic particles and heavy metals in the road dust: Magnetic identification and its implications, *Atmos. Environ.*, *44*(9), 1175–1185.

Yunker, M. B., R. W. Macdonald, R. Vingarzan, R. H. Mitchell, D. Goyette, and S. Sylvestre (2002), PAHs in the Fraser River basin: A critical appraisal of PAH ratios as indicators of PAH source and composition, *Org. Geochem.*, *33*, 489–515.

Zhang, X. Y., R. Arimoto, G. H. Zhu, T. Chen, and G. Y. Zhang (1998), Concentration, size-distribution and deposition of mineral aerosol over Chinese desert regions, *Tellus, Ser. B*, *50*, 317–330.